

**1 Measurement of the Drell-Yan Absolute Cross-Section
2 in pp and pd Collisions with a 120 GeV Proton Beam at
3 Fermilab**

4 Chatura Kuruppu¹, Stephen Pate¹

5 ¹New Mexico State University, Las Cruces, NM 88003, USA

6 February 11, 2026

7 Abstract

This analysis note reports on the determination of pp and pd Drell-Yan absolute cross sections from data collected using the Roadset 67 trigger. We seek preliminary approval of these results for presentation in upcoming conferences. This work extends previous analyses by incorporating both Liquid Hydrogen (LH_2) and Liquid Deuterium (LD_2) target data. Furthermore, significant updates to the efficiency corrections have been implemented. The reconstruction efficiency is now calculated using a global curve based on the $D1$ occupancy variable, integrated over all kinematic bins, as demonstrated in DocDB 11427. Additionally, the hodoscope efficiency correction has been upgraded from a constant factor to a dimuon-level calculation using RoadIDs and paddle-specific efficiencies (DocDB 11467). In this work, we report the measurement of the double-differential Drell-Yan cross-sections, $d^2\sigma/dx_F dM$, and compare the results with theoretical predictions from Quantum Chromodynamics (QCD).

20 This work was supported in part by US DOE grant DE-FG02-94ER40847.

21 Contents

22	1 Introduction	5
23	2 Analysis Methodology	5
24	2.1 Data and Monte Carlo Samples	5
25	2.2 Event Selection	6
26	2.3 Cross-Section Formalism	7
27	3 Acceptance and Efficiency Corrections	9
28	3.1 Detector Acceptance Correction	9
29	4 Reconstruction Efficiency Correction	26
30	4.1 Uncertainty Propagation	27
31	5 Hodoscope Efficiency Correction	27
32	6 Total Efficiency Correction	32
33	7 Determination of Corrected Yields	34
34	8 Appendix: Event Selection Criteria (Chuck Cuts)	36
35	8.1 Single Track Cuts	36
36	8.2 Dimuon Cuts	36
37	8.3 Occupancy and Topology Cuts	36
38	9 Appendix: Efficiency Plots	38
39	10 Appendix: Table of Systematic Errors	39
40	11 Appendix: Table of Cross-Section Values	43
41	12 Appendix: Transverse Momentum Distributions	47

42 List of Figures

43 1	Dimuon distributions after applying event selection criteria.	8
44 2	Acceptance plots for $0.00 \leq x_F < 0.05$	10
45 3	Acceptance plots for $0.05 \leq x_F < 0.10$	11
46 4	Acceptance plots for $0.10 \leq x_F < 0.15$	12
47 5	Acceptance plots for $0.15 \leq x_F < 0.20$	13
48 6	Acceptance plots for $0.20 \leq x_F < 0.25$	14
49 7	Acceptance plots for $0.25 \leq x_F < 0.30$	15
50 8	Acceptance plots for $0.30 \leq x_F < 0.35$	16
51 9	Acceptance plots for $0.35 \leq x_F < 0.40$	17
52 10	Acceptance plots for $0.40 \leq x_F < 0.45$	18
53 11	Acceptance plots for $0.45 \leq x_F < 0.50$	19
54 12	Acceptance plots for $0.50 \leq x_F < 0.55$	20
55 13	Acceptance plots for $0.55 \leq x_F < 0.60$	21
56 14	Acceptance plots for $0.60 \leq x_F < 0.65$	22
57 15	Acceptance plots for $0.65 \leq x_F < 0.70$	23
58 16	Acceptance plots for $0.70 \leq x_F < 0.75$	24
59 17	Acceptance plots for $0.75 \leq x_F < 0.80$	25
60 18	Global Reconstruction Efficiency curve as a function of the $D1$ occupancy variable, integrated over all kinematic bins.	26
61 19	Average Reconstruction Efficiencies calculated each kinematic bin with the prop- agated uncertainties.	28
62 20	Hodoscope Paddle Efficiencies calculated in each plane.	29
63 21	Hodoscope Paddle hit distributions arranged by Plane (Rows 1-4), Top vs Bottom. .	30
64 22	Average Hodoscope Efficiencies calculated each kinematic bin with the propagated uncertainties.	31
65 23	Average total Efficiencies calculated each kinematic bin with the propagated un- certainties.	33
66 24	Average efficiency correction for signal and final corrected yields.	35

71 List of Tables

72 1	Single track selection criteria.	36
73 2	Dimuon kinematic and vertex selection criteria.	37
74 3	Occupancy and topological cuts.	37
75 4	Detailed Systematic Error calculation for Bins in x_F and Mass	39
76 5	Detailed cross-section calculation for Bins in x_F and Mass	43

77 1 Introduction

78 The Drell-Yan process, where a quark from one hadron annihilates with an antiquark from
79 another to produce a lepton-antilepton pair ($q\bar{q} \rightarrow \ell^+\ell^-$), provides a clean and direct probe
80 of the antiquark structure of nucleons. Over the past several decades, Drell-Yan experiments
81 have been instrumental in mapping the parton distribution functions (PDFs) of the proton and
82 other hadrons. However, most existing data are concentrated at small to moderate values of
83 the parton momentum fraction, $x < 0.3$. The region of large x ($x > 0.3$) remains relatively
84 unexplored, yet it is crucial for understanding phenomena such as the flavor asymmetry of the
85 proton's light antiquark sea ($\bar{d}(x)/\bar{u}(x)$) and the fundamental mechanisms of non-perturbative
86 QCD that govern hadron structure.

87 The SeaQuest experiment (E906) at Fermilab was designed specifically to explore this high- x
88 frontier. By impinging a high-intensity 120 GeV proton beam from the Main Injector onto various
89 fixed targets, including liquid hydrogen (LH_2) and liquid deuterium (LD_2), SeaQuest measures
90 dimuon production in a kinematic region sensitive to antiquarks carrying a large fraction of the
91 nucleon's momentum.

92 This analysis presents a measurement of the absolute double-differential Drell-Yan cross-
93 section, binned in the dimuon invariant mass (M) and Feynman- x (x_F), using data collected
94 with the LH_2 and LD_2 targets. The p+p collisions are primarily sensitive to the \bar{u} distribution
95 in the proton, while the p+d collisions provide information on the sum of \bar{u} and \bar{d} . These results
96 provide stringent new constraints on modern PDF parameterizations in the valence-dominated
97 region.

98 The cross-section is presented in its scaling form, which, in the leading-order Drell-Yan
99 model, is independent of the center-of-mass energy, \sqrt{s} :

$$100 M^3 \frac{d^2\sigma}{dMdx_F} = f(\tau) \quad (1)$$

101 where $\tau = M^2/s$. The experimental determination of this quantity requires a precise under-
102 standing of the integrated luminosity, detector acceptance, and reconstruction efficiencies, which
103 are detailed in the subsequent sections of this document.

103 2 Analysis Methodology

104 The extraction of the Drell-Yan cross-section from the raw data involves several distinct steps:
105 selecting candidate dimuon events, subtracting backgrounds, calculating the integrated luminos-
106 ity, and correcting for detector- and reconstruction-related inefficiencies.

107 2.1 Data and Monte Carlo Samples

108 This analysis utilizes the “Roadset 67” dataset collected by the SeaQuest experiment. The
109 primary data files for the liquid hydrogen (LH_2) target and the corresponding empty “flask”
110 target runs are saved in:

```
111 /seaquest/users/apun/e906_projects/rs67_merged_files/  
112 • Data ( $LH_2$  Target): merged_RS67_3089LH2.root  
113 • Data ( $LD_2$  Target): merged_RS67_3089LD2.root  
114 • Background (Empty Flask): merged_RS67_3089Flask.root
```

115 To properly correct for detector performance, we calculate the hodoscope and reconstruction
116 efficiency corrections at the dimuon level. The above ROOT files were modified by adding the
117 following variables to each event:

```

118 • recoeff: reconstruction efficiency correction
119 • recoeff_error: propagated uncertainty of the reconstruction efficiency correction
120 • hodoeff: hodoscope efficiency correction
121 • hodoeff_error: propagated uncertainty of the hodoscope efficiency correction
122
123 The updated datasets containing these variables are saved in the following locations:
124
125 • /seaquest/users/ckuruppu/rootfiles/rs67/merged_RS67_3089_LH2_recoeff_hodoeff.root
126 • /seaquest/users/ckuruppu/rootfiles/rs67/merged_RS67_3089_LD2_recoeff_hodoeff.root
127 • /seaquest/users/ckuruppu/rootfiles/rs67/merged_RS67_3089_Flask_recoeff_hodoeff.root
128
129 The empty flask data are crucial for subtracting contributions from beam interactions with
130 the target vessel walls and other upstream material.
131 To correct for detector acceptance and reconstruction efficiencies, extensive Monte Carlo
132 (MC) simulations were employed. The simulations model the Drell-Yan process and propagate
133 the resulting muons through a Geant4-based model of the SeaQuest spectrometer. The primary
134 MC files used are:
135
136 • Acceptance Study: Drell-Yan events were generated over a  $4\pi$  solid angle (“thrown”) and
137 also processed through the full detector simulation and reconstruction chain (“accepted”). This
138 study uses the *_M027_S001_* series of files saved in:
139
140     /seaquest/users/chleung/pT_ReWeight/
141
142     – mc_drellyan_LH2_M027_S001_4pi_pTxFweight_v2.root
143     – mc_drellyan_LH2_M027_S001_clean_occ_pTxFweight_v2.root
144     – mc_drellyan_LH2_M027_S001_messy_occ_pTxFweight_v2.root
145     – mc_drellyan_LD2_M027_S001_4pi_pTxFweight_v2.root
146     – mc_drellyan_LD2_M027_S001_clean_occ_pTxFweight_v2.root
147     – mc_drellyan_LD2_M027_S001_messy_occ_pTxFweight_v2.root
148
149 • Efficiency Study: To model the effect of high detector occupancy on track reconstruction,
150 simulated events were processed with (“messy”) and without (“clean”) the overlay of random
151 background hits from experimental data. This study uses the *_M027_S001_* series of files
152 also saved in the same location.
153
154 All MC samples are weighted on an event-by-event basis to match the transverse momentum
155 ( $p_T$ ) distribution observed in the data.
156
157 

## 2.2 Event Selection


158
159 A multi-tiered set of selection criteria is applied to isolate high-quality Drell-Yan dimuon events
160 from the large background of other processes.
161
162 • Data Quality: Only data from “good spills,” as identified by standard run quality monitoring,
163 are included in the analysis. A physics trigger condition (MATRIX1 == 1) is required,
164 selecting events consistent with the passage of two muons through the spectrometer.

```

155 • **Track and Dimuon Quality:** A set of stringent cuts, developed by the collaboration and
 156 referred to as “Chuck cuts,” are applied to ensure well-reconstructed positive and negative
 157 muon tracks that form a high-quality common vertex. These cuts impose requirements on
 158 track χ^2 , momentum, number of hits, and fiducial volume. The full details of these cuts
 159 are provided in Appendix 8.

160 • **Kinematic Selection:** The analysis focuses on the high-mass continuum, away from the
 161 charmonium resonances ($J/\psi, \psi'$). A cut of $M_{\mu\mu} > 4.2$ GeV is applied. The analysis is
 162 restricted to the kinematic range $0 < x_F < 0.8$.

163 After applying the event selection criteria mentioned in the Appendix, the total and mix
 164 yields for the LH₂, LD₂, and Empty Flask targets in each kinematic bin are extracted. The
 165 distributions are shown in Figure 1.

166 2.3 Cross-Section Formalism

167 The double-differential cross-section in a given kinematic bin ($\Delta M, \Delta x_F$) is calculated as (refer
 168 DocDB 11445-V3):

$$\frac{d^2\sigma}{dMdx_F} = \frac{1}{\epsilon_{\text{acc}}\Delta M\Delta x_F} \left[\frac{Y_{\text{total}}^{\text{LH2}} - Y_{\text{mixed}}^{\text{LH2}}}{\epsilon_{\text{signal}}^{\text{LH2}}} - \frac{I_{\text{LH2}}}{I_{\text{flask}}} \left(\frac{Y_{\text{total}}^{\text{flask}} - Y_{\text{mixed}}^{\text{flask}}}{\epsilon_{\text{signal}}^{\text{flask}}} \right) \right] \quad (2)$$

169 where:

- 170 • $Y_{\text{total}}^{\text{LH2}}$ is the total LH2 target dimuon yield after the event selection criteria.
- 171 • $Y_{\text{mixed}}^{\text{LH2}}$ is the estimated mixed background yield from mixed events for the LH2 target.
- 172 • $Y_{\text{total}}^{\text{flask}}$ is the total flask target dimuon yield after the event selection criteria.
- 173 • $Y_{\text{mixed}}^{\text{flask}}$ is the estimated mixed background yield from mixed events for the flask target.
- 174 • $\epsilon_{\text{signal}}^{\text{LH2}}$ is the average signal efficiency correction for the LH2 target dimuons.
- 175 • $\epsilon_{\text{signal}}^{\text{flask}}$ is the average signal efficiency correction for the flask target dimuons.
- 176 • \mathcal{L} is the integrated luminosity for the dataset.

177 The average signal efficiency correction can be calculated as:

$$\epsilon_{\text{signal}} = \frac{1}{Y_{\text{total}} - Y_{\text{mixed}}} [\epsilon_{\text{total}} Y_{\text{total}} - \epsilon_{\text{mixed}} Y_{\text{mixed}}] \quad (3)$$

178 where:

- 179 • ϵ_{total} is the average total efficiency correction for the total yield.
- 180 • ϵ_{mixed} is the average mixed efficiency correction for the mixed background yield.

181 as explained in DocDB 11448-V2.

182 In each case, efficiency correction of the i^{th} dimuon is defined as:

$$\epsilon^i = \epsilon_{\text{recon}}^i \cdot \epsilon_{\text{hodo}}^i \quad (4)$$

183 where $\epsilon_{\text{recon}}^i$ is the reconstruction efficiency for the i^{th} dimuon and ϵ_{hodo}^i is the hodoscope effi-
 184 ciency for the i^{th} dimuon.

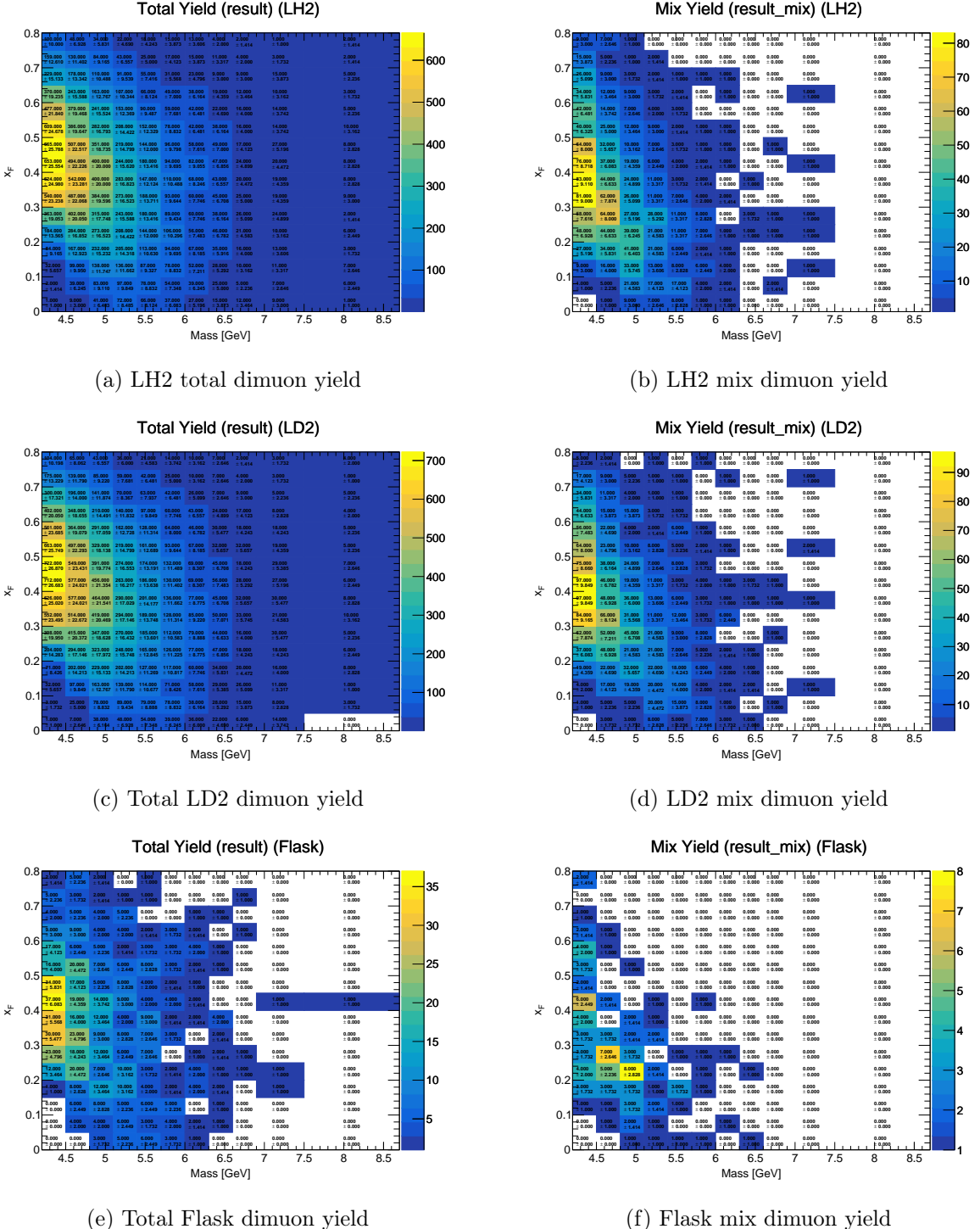


Figure 1: Dimuon distributions after applying event selection criteria.

The integrated luminosity, \mathcal{L} , is given by the product of the total number of protons incident on the target and the number of target nuclei per unit area:

$$\mathcal{L} = N_{\text{incident}} \cdot \frac{N_A \rho L}{A} \cdot f_{\text{atten}} \quad (5)$$

Here, N_{incident} is the number of protons on target, N_A is Avogadro's number, ρ is the target density, L is the target length, A is the molar mass, and f_{atten} is a correction factor for beam attenuation within the thick target. For the $L = 50.8$ cm long LH₂ target, with a density of

¹⁹⁰ $\rho_H = 0.0708 \text{ g/cm}^3$, the target thickness is 3.5966 g/cm^2 with a beam attenuation factor of
¹⁹¹ 0.966.

¹⁹² The total correction factor, ϵ_{total} , is the product of three terms determined from MC simu-
¹⁹³ lations:

$$\epsilon_{\text{total}} = \epsilon_{\text{acc}}(M, x_F) \cdot \epsilon_{\text{recon}}(M, x_F) \cdot \epsilon_{\text{trigger}} \quad (6)$$

¹⁹⁴ where ϵ_{acc} is the geometric and kinematic acceptance of the spectrometer, ϵ_{recon} is the track
¹⁹⁵ reconstruction efficiency (often called “kTracker efficiency”), and $\epsilon_{\text{trigger}}$ is the trigger efficiency.
¹⁹⁶ The calculation of these three terms is detailed in the following sections.

¹⁹⁷ 3 Acceptance and Efficiency Corrections

¹⁹⁸ 3.1 Detector Acceptance Correction

¹⁹⁹ The SeaQuest spectrometer has a finite geometric acceptance, which limits the fraction of pro-
²⁰⁰ duced dimuon events that can be detected. This acceptance depends strongly on the event
²⁰¹ kinematics, primarily the dimuon invariant mass (M) and Feynman- x (x_F). The acceptance
²⁰² correction factor is determined using MC simulations.

²⁰³ The acceptance, $A(M, x_F)$, is defined as the ratio of the number of simulated events that
²⁰⁴ are successfully reconstructed and pass all analysis cuts (N_{reco}) to the total number of events
²⁰⁵ generated in a given kinematic bin (N_{gen}):

$$\text{Acceptance (A)} = \frac{N_{\text{reco}}}{N_{\text{gen}}} \quad (7)$$

²⁰⁶ This calculation is performed in bins of M and x_F . The kinematic binning used for this study
²⁰⁷ is defined by the following edges:

- ²⁰⁸ • x_F Edges: $\{0, 0.05, 0.1, \dots, 0.8\}$ (16 bins)
- ²⁰⁹ • Mass Edges (GeV/c^2): $\{4.2, 4.5, 4.8, 5.1, 5.4, 5.7, 6, 6.3, 6.6, 6.9, 7.5, 8.7\}$ (11 bins)

²¹⁰ The following pages show the calculated acceptance as a function of mass for each of the
²¹¹ 16 x_F bins. The plots show the acceptance for the LH₂ and LD₂ targets, their combined
²¹² average, and their ratio. The ratio is close to unity across the kinematic range, indicating that
²¹³ target-dependent effects on the acceptance are small. In this case, we compare newly calculated
²¹⁴ acceptance corrections to the existing acceptance calculations saved in Shivangi’s file:

²¹⁵ `./shivangi/work/analysis/R008/diffCross/v42/5770/looseCut/final/acceptance_h.root`

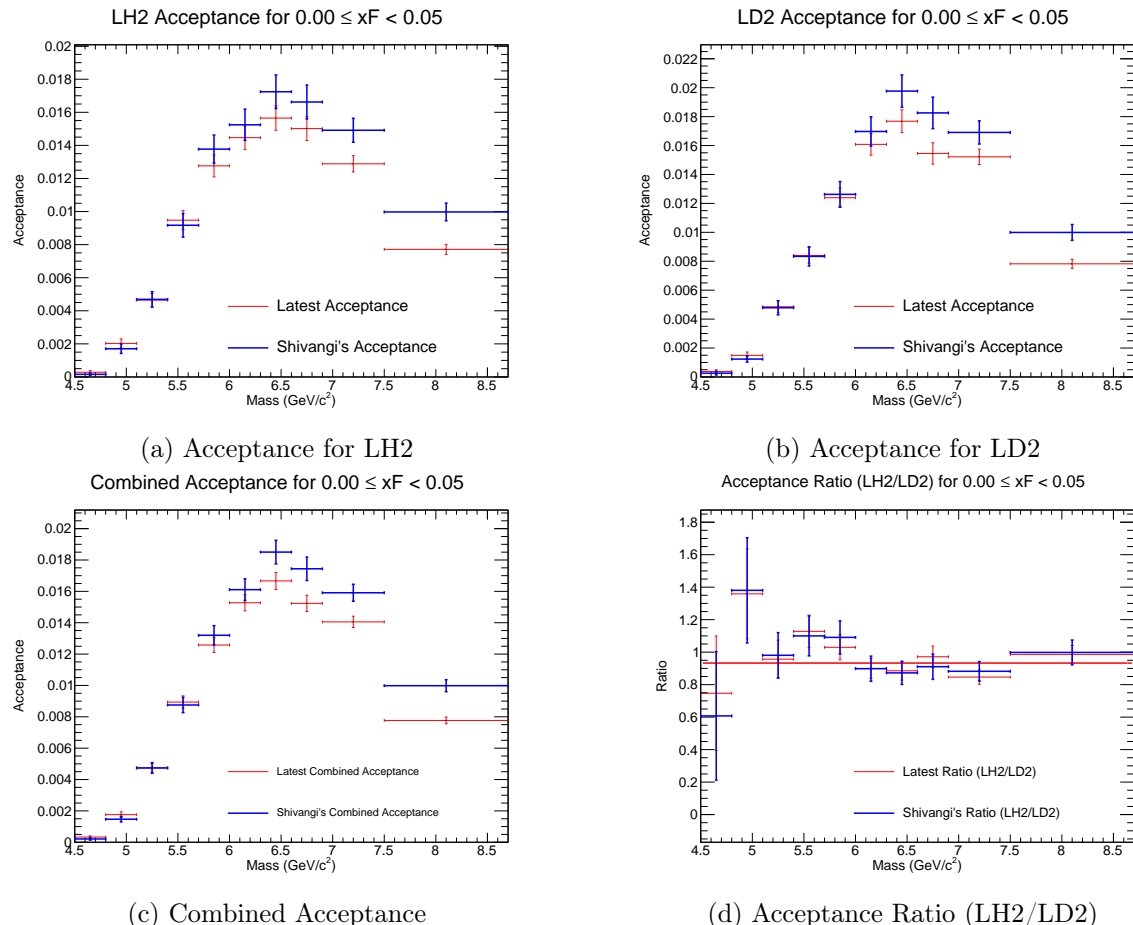


Figure 2: Acceptance plots for $0.00 \leq x_F < 0.05$.

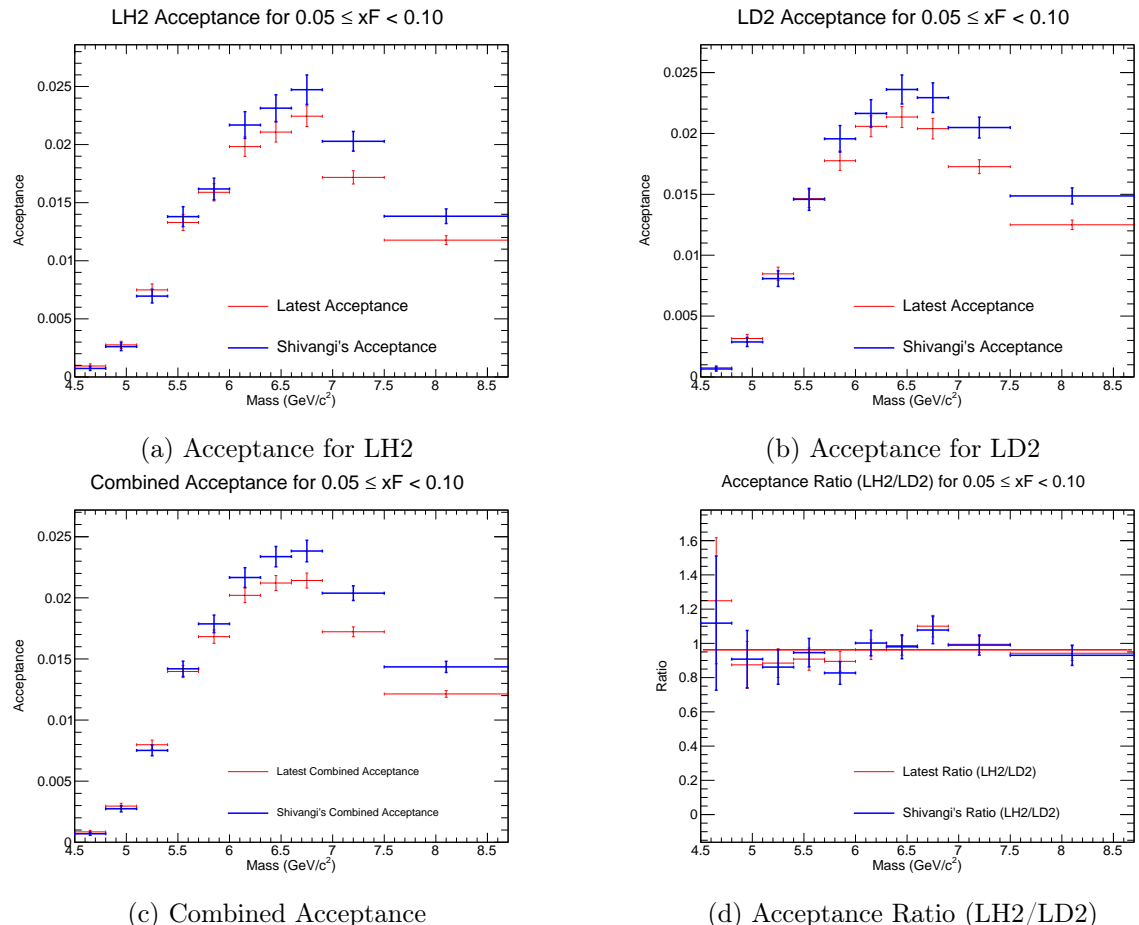


Figure 3: Acceptance plots for $0.05 \leq x_F < 0.10$.

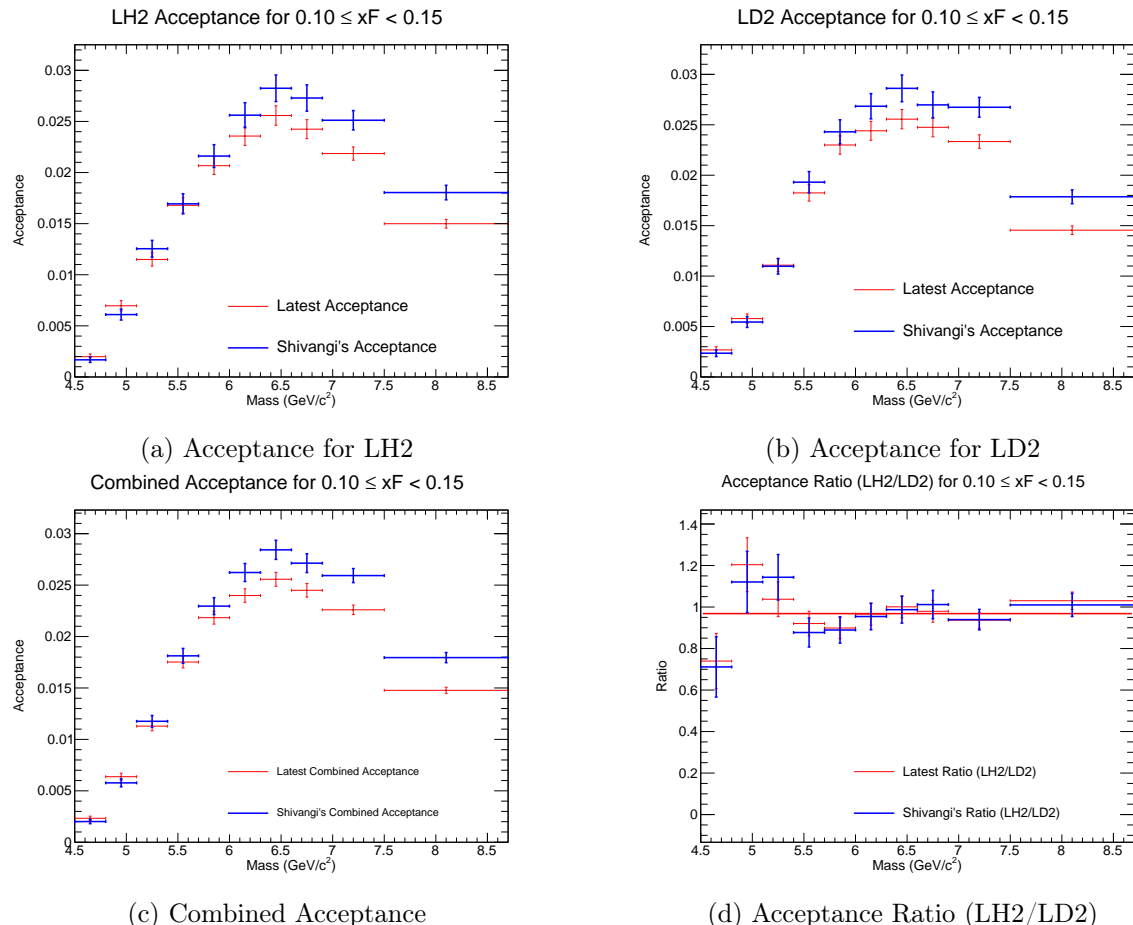


Figure 4: Acceptance plots for $0.10 \leq x_F < 0.15$.

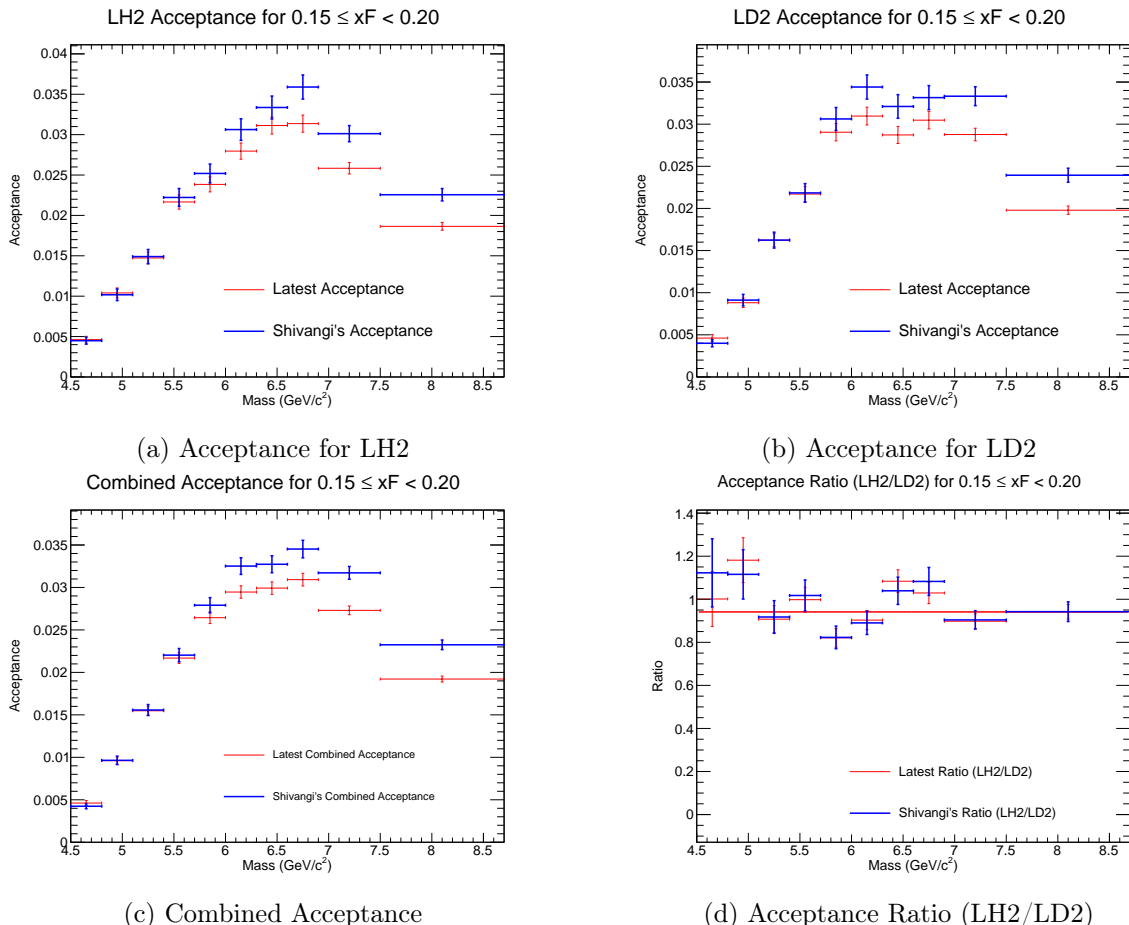


Figure 5: Acceptance plots for $0.15 \leq x_F < 0.20$.

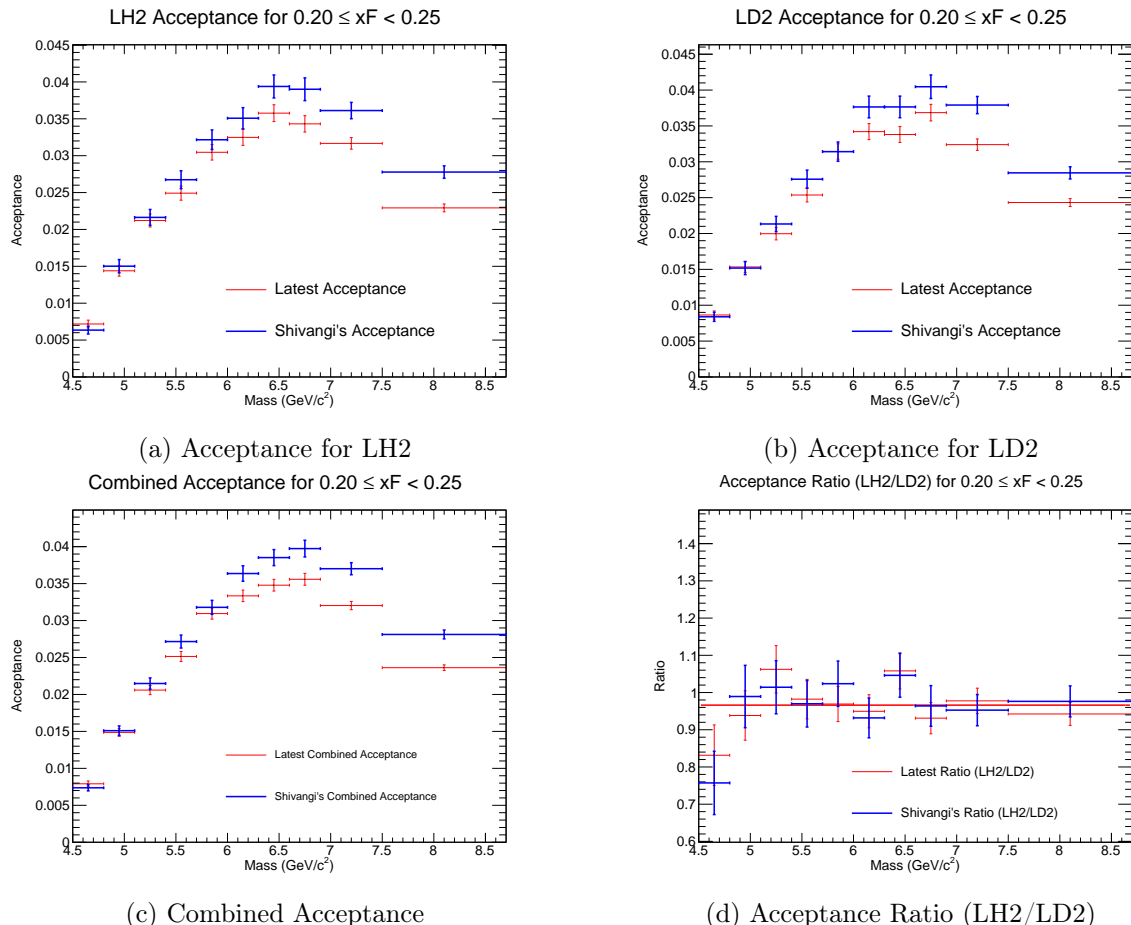


Figure 6: Acceptance plots for $0.20 \leq x_F < 0.25$.

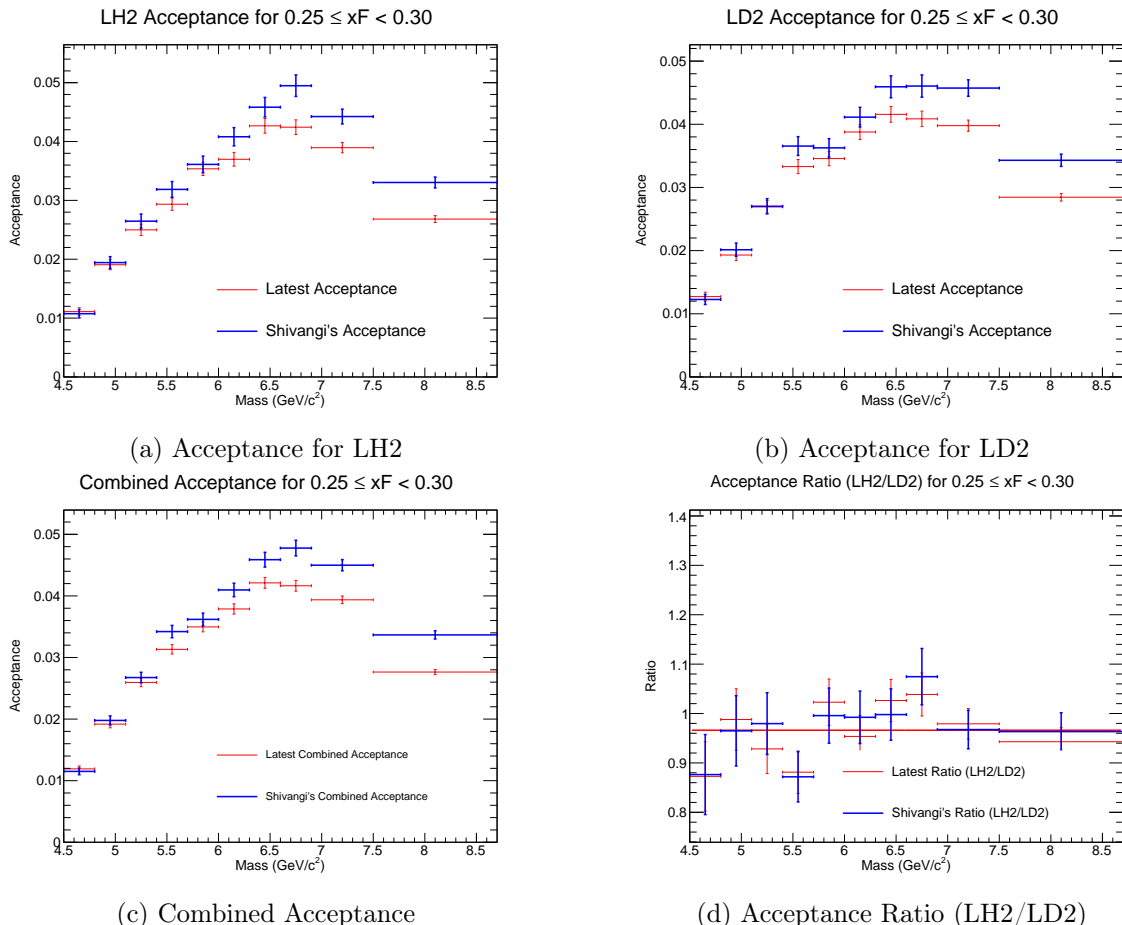


Figure 7: Acceptance plots for $0.25 \leq x_F < 0.30$.

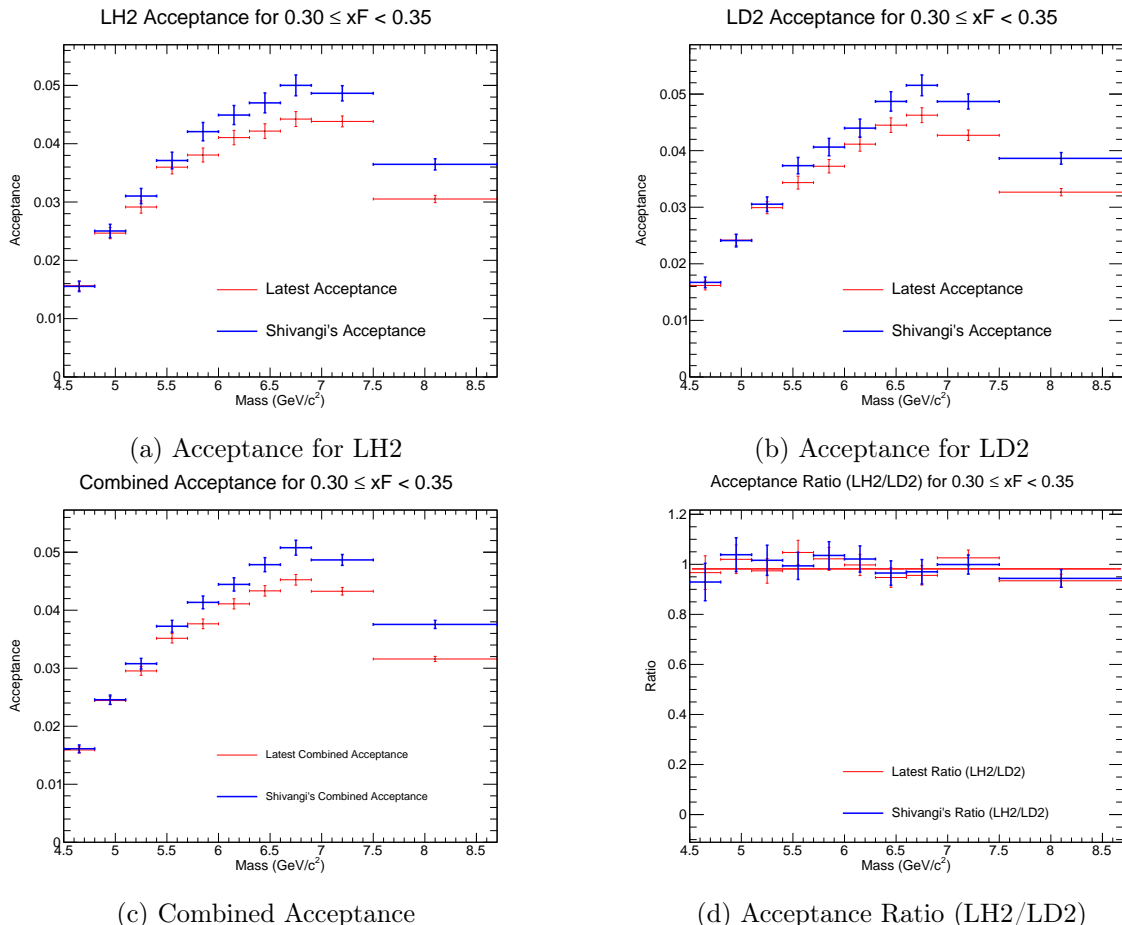


Figure 8: Acceptance plots for $0.30 \leq x_F < 0.35$.

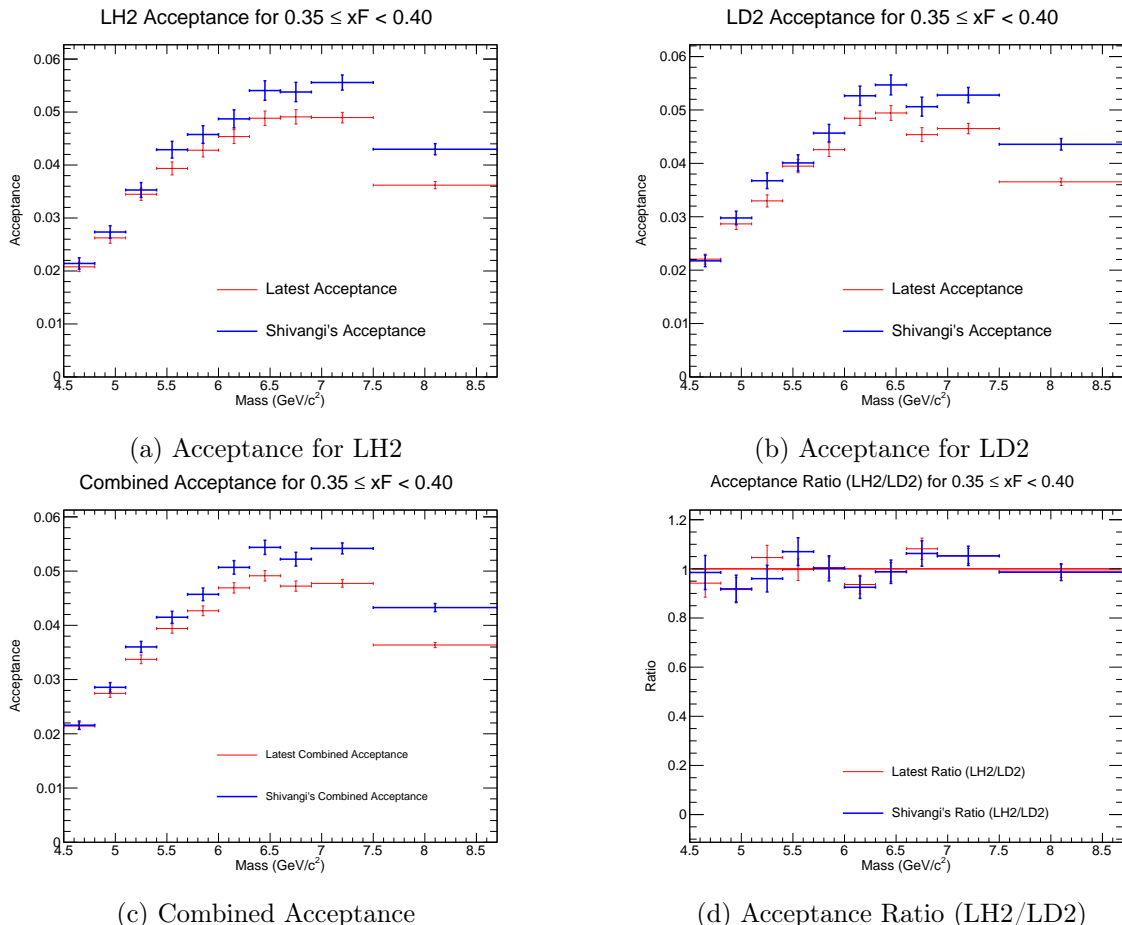


Figure 9: Acceptance plots for $0.35 \leq x_F < 0.40$.

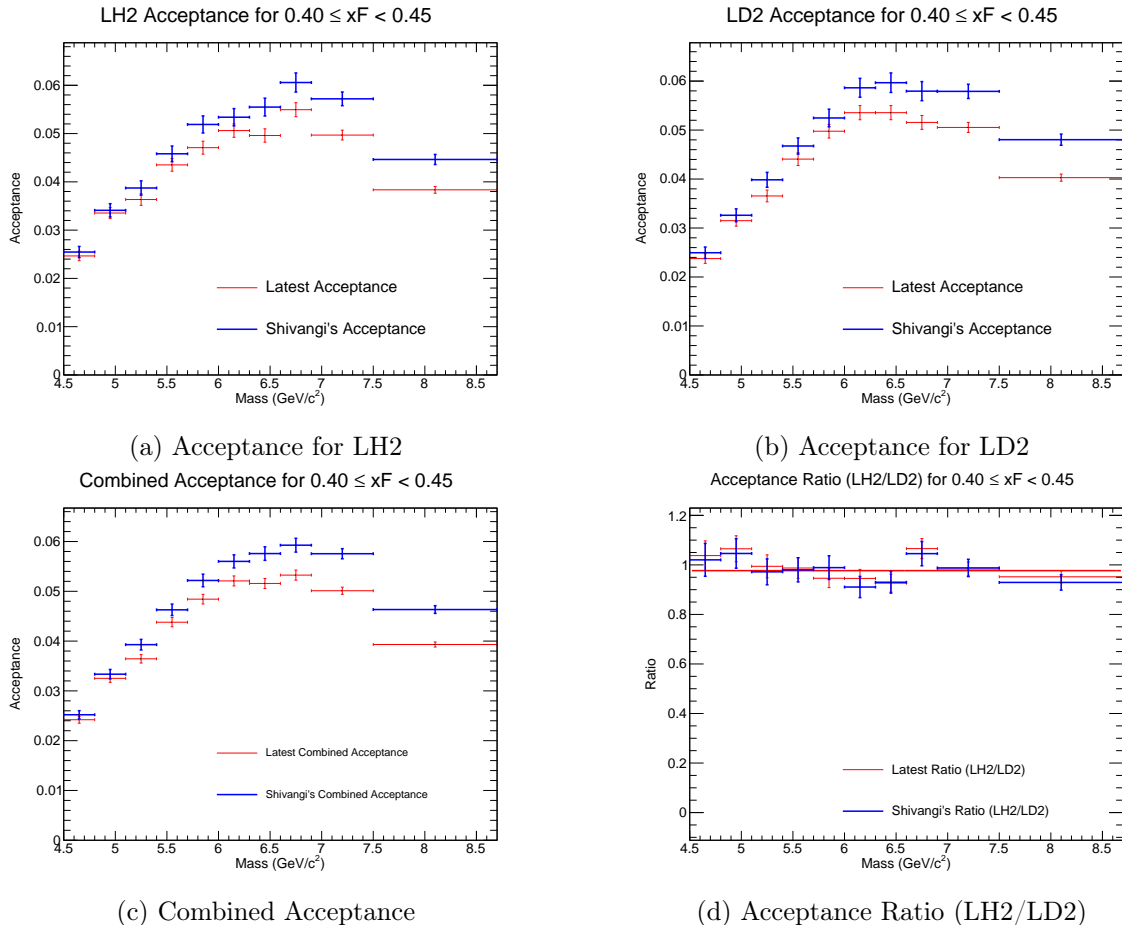


Figure 10: Acceptance plots for $0.40 \leq x_F < 0.45$.

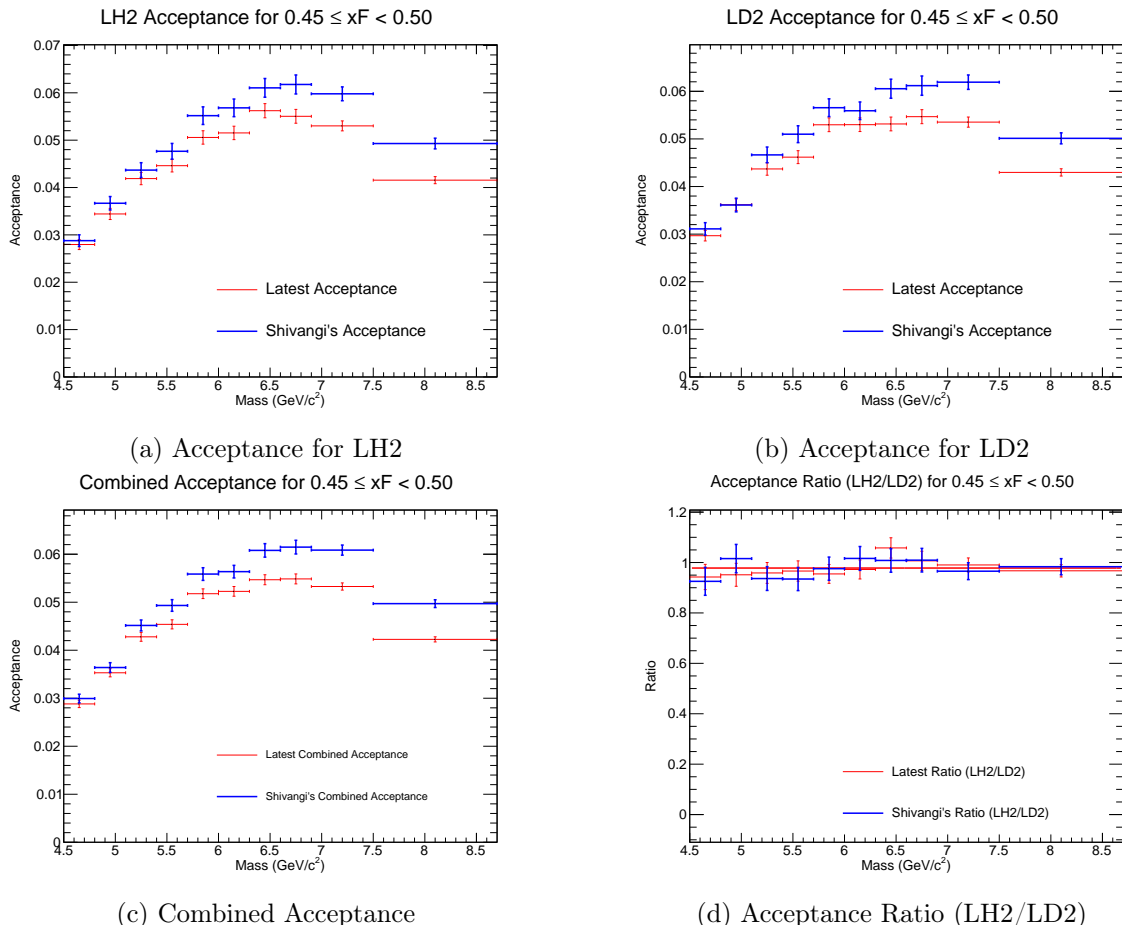


Figure 11: Acceptance plots for $0.45 \leq x_F < 0.50$.

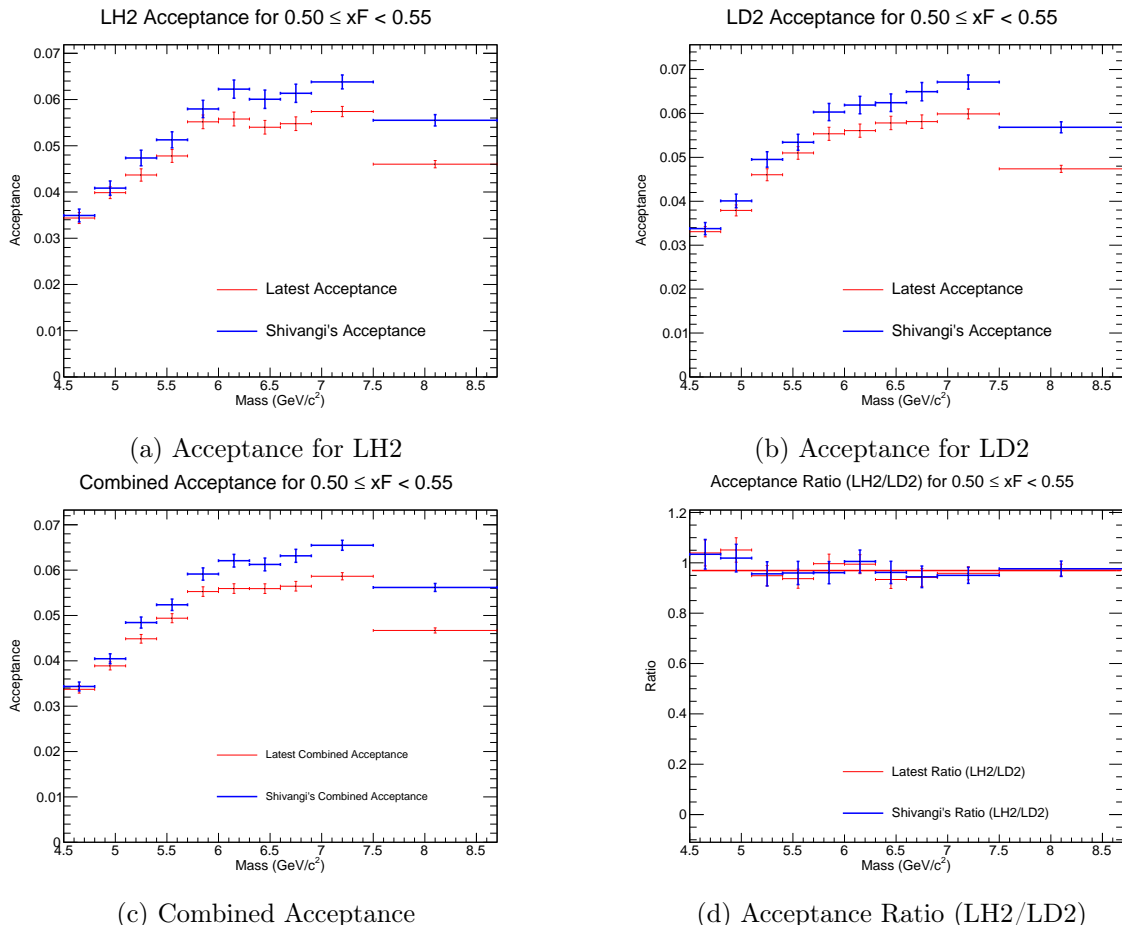


Figure 12: Acceptance plots for $0.50 \leq x_F < 0.55$.

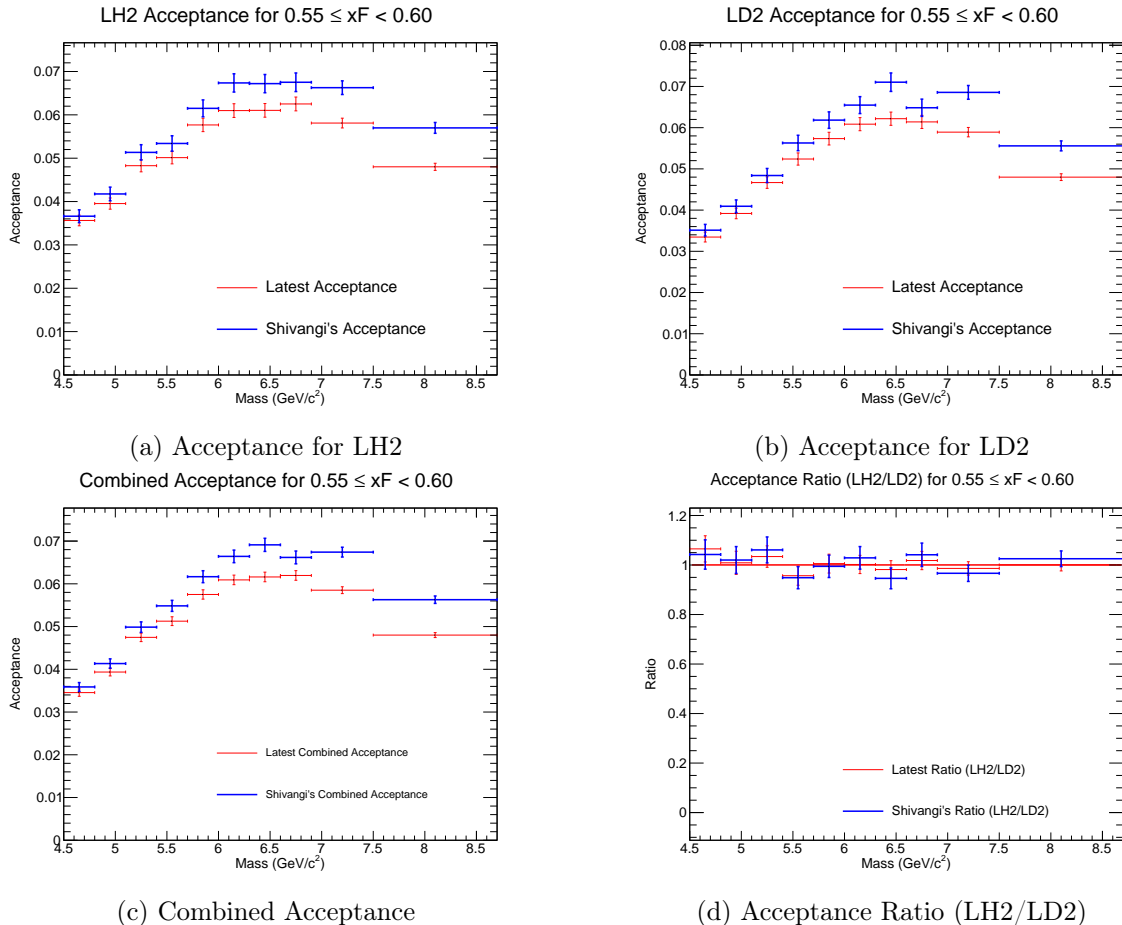


Figure 13: Acceptance plots for $0.55 \leq x_F < 0.60$.

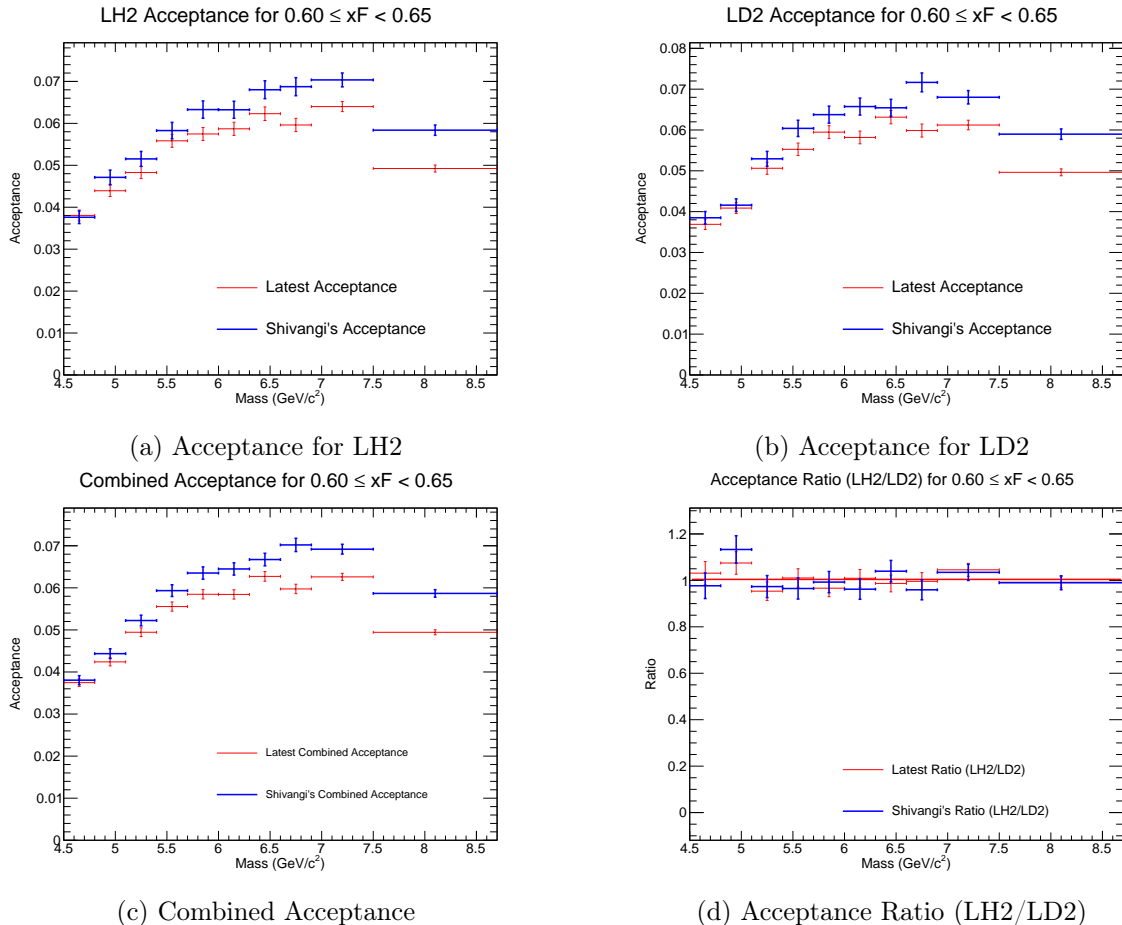


Figure 14: Acceptance plots for $0.60 \leq x_F < 0.65$.

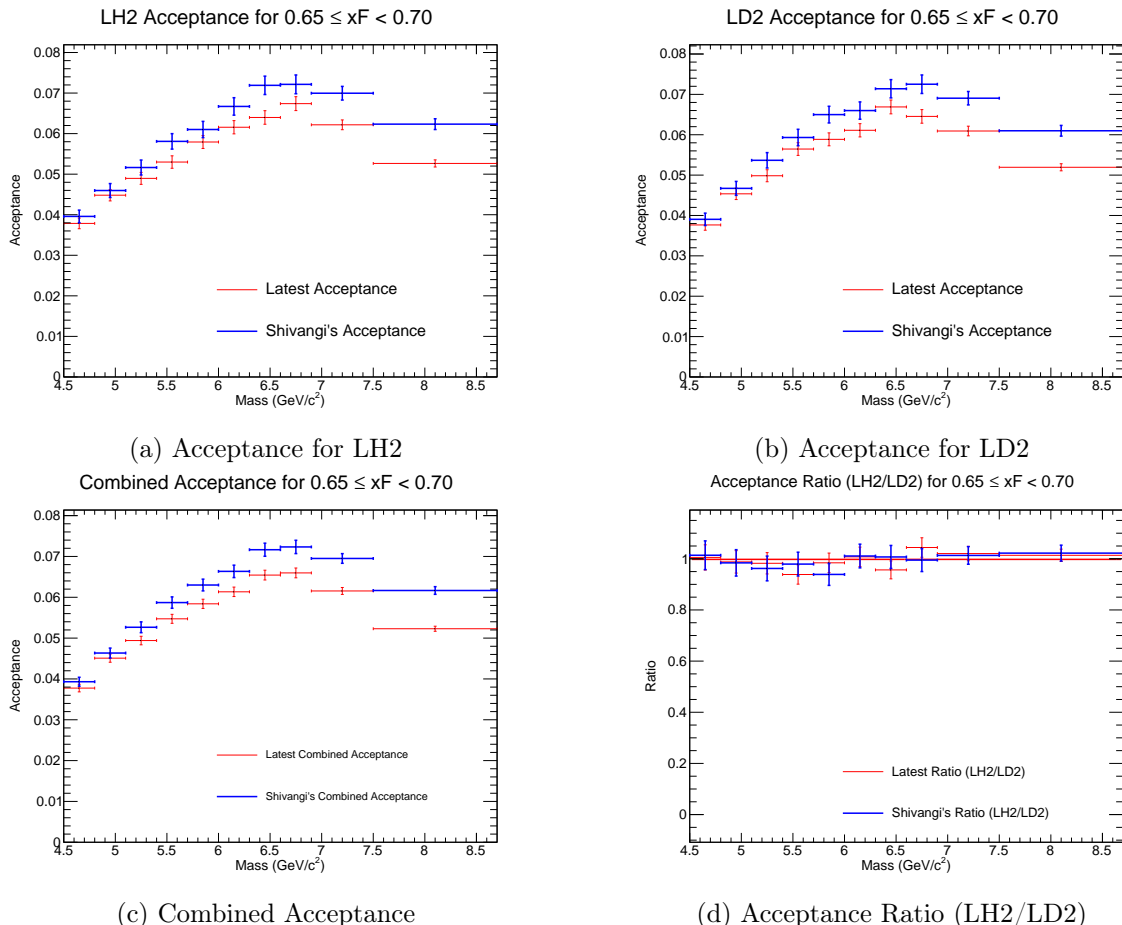


Figure 15: Acceptance plots for $0.65 \leq x_F < 0.70$.

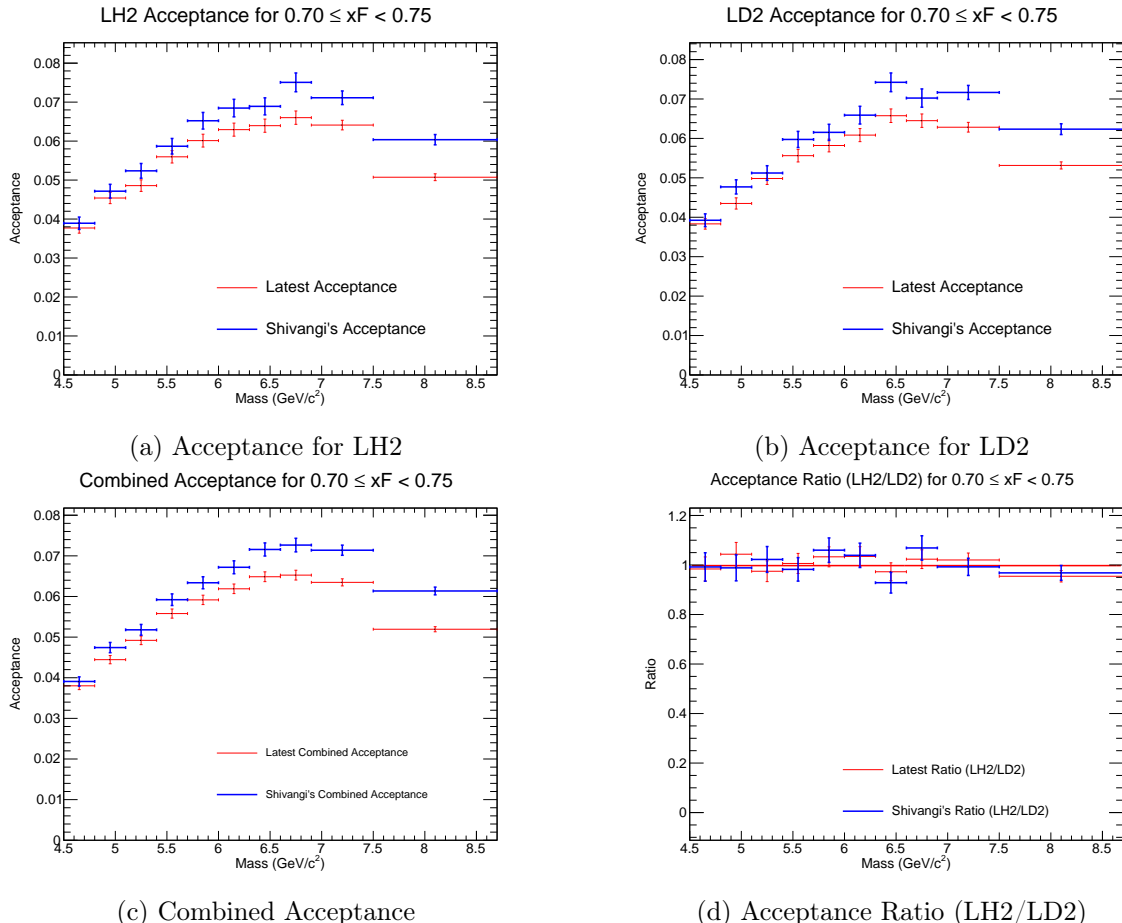


Figure 16: Acceptance plots for $0.70 \leq x_F < 0.75$.

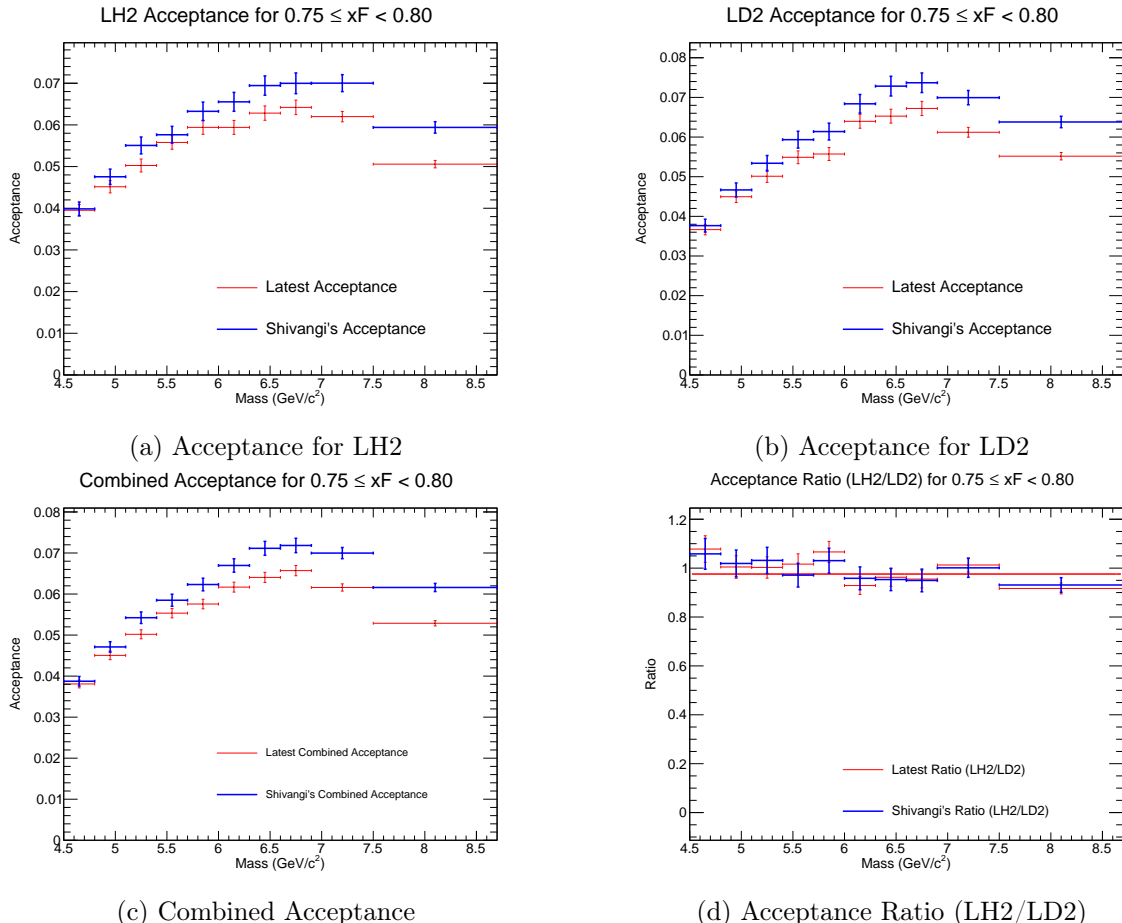


Figure 17: Acceptance plots for $0.75 \leq x_F < 0.80$.

216 4 Reconstruction Efficiency Correction

217 The track-finding algorithm (“kTracker”) has an efficiency that depends on the detector occu-
 218 pancy; the number of hits in the detector during an event. This efficiency is studied using
 219 “clean” MC simulations (signal only) and “messy” MC simulations (signal with background hits
 220 overlaid). The reconstruction efficiency, ϵ_{recon} , is defined as the ratio of events found in the
 221 messy sample to those in the clean sample, as a function of an occupancy-related variable (e.g.,
 222 D2, the number of hits in Drift Chamber Station 2).

$$\epsilon_{\text{recon}}(\text{D1}) = \frac{N_{\text{reco}}^{\text{messy}}(\text{D1})}{N_{\text{reco}}^{\text{clean}}(\text{D1})} \quad (8)$$

223 We have updated the reconstruction efficiency calculation compared to previous reconstruc-
 224 tion efficiency calculation. Previously, reconstruction efficiency was calculated by creating curves
 225 in each kinematic bin using the $D2$ occupancy variable. However, it has been demonstrated that
 226 there is little correlation between reconstruction efficiency and different kinematic bins (DocDB
 227 11427). Therefore, we utilize a **global reconstruction efficiency curve**, defined with efficiency
 228 on the y-axis and the $D1$ **occupancy variable** on the x-axis, integrated over all kinematic bins.

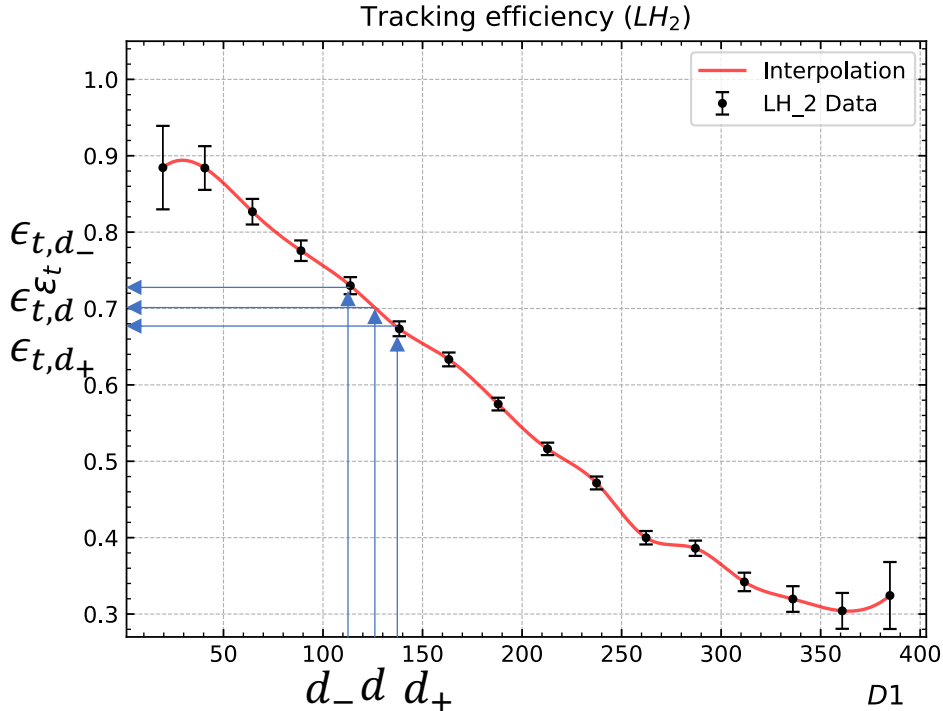


Figure 18: Global Reconstruction Efficiency curve as a function of the $D1$ occupancy variable, integrated over all kinematic bins.

229 For each dimuon passing event selection, the reconstruction efficiency is calculated based on
 230 its $D1$ occupancy using following equation:

$$\epsilon_i = \epsilon(D1^-) + \left(\frac{\epsilon(D1^+) - \epsilon(D1^-)}{D1^+ - D1^-} \right) (D1^+ - D1_i) \quad (9)$$

231 where $D1_i$ is the $D1$ occupancy for the dimuon event, and $D1^-$ and $D1^+$ are the nearest lower
 232 and upper bin edges on the global reconstruction efficiency curve. For **mixed events**, the
 233 reconstruction efficiency is calculated using an average $D1$ occupancy:

$$D1_{\text{mixed}} = \frac{D1_{\text{pos}} + D1_{\text{neg}}}{2} \quad (10)$$

234 An average reconstruction efficiency, $\langle\epsilon_{\text{recon}}\rangle$, with correctly propagated uncertainty, is then
 235 calculated for each kinematic bin. The Global Reconstruction Efficiency curve and the 2-D
 236 plots of the average efficiency for LH2 target dimuons and LH2 mixed events are presented
 237 below.

238 4.1 Uncertainty Propagation

239 An important aspect of this procedure is the correct propagation of uncertainties. For each event
 240 in the data with a measured D1 value, an efficiency ϵ_i and its uncertainty $\delta\epsilon_i$ are determined by
 241 linear interpolation between points on the MC-derived efficiency curve. For a given event i the
 242 efficiency will be interpolated:

$$\delta\epsilon_i = \frac{1}{D1^+ - D1^-} \sqrt{(D1^+ - D1_i)^2 \delta\epsilon(D1^+)^2 + (D1^- - D1_i)^2 \delta\epsilon(D1^-)^2} \quad (11)$$

243 where $D1_i$ is the value of D1 for the event i , $D1^+$ is the nearest D1 value greater than $D1_i$,
 244 $D1^-$ is the nearest D1 value less than $D1_i$, $\epsilon(D1^\pm)$ is the value of the efficiency at $D1^\pm$, and
 245 $\delta\epsilon(D1^\pm)$ is the uncertainty in $\epsilon(D1^\pm)$.

246 The average efficiency $\langle\epsilon\rangle$ for a bin containing N data events is the mean of the individual
 247 efficiencies:

$$\langle\epsilon\rangle = \frac{1}{N} \sum_{i=1}^N \epsilon_i \quad (12)$$

248 The uncertainty on this average, $\delta\langle\epsilon\rangle$, is based on the propagated error from the uncertainty
 249 on the MC-derived efficiency curve itself.

$$\delta_{\text{prop}}\langle\epsilon\rangle = \frac{1}{N} \sqrt{\sum_{i=1}^N (\delta\epsilon_i)^2} \quad (13)$$

250 We calculate the average reconstruction efficiency and its propagated uncertainty for both
 251 target dimuons and mixed dimuons in each kinematic bin. The average reconstruction efficiency
 252 correction calculated for each kinematic bin with the propagated uncertainty for target dimuons
 253 and mixed events are shown in 2-D plots below in Figure 19.

254 5 Hodoscope Efficiency Correction

255 Previously, a constant hodoscope efficiency correction of 0.845 ± 0.125 was used (DocDB 11383-v4). In this analysis, we calculate the hodoscope efficiency for both target dimuons and mixed
 256 dimuons on an event-by-event basis. This is done by determining the roadID for the positive track
 257 ('posRoad') and the negative track ('negRoad') and utilizing the hodoscope paddle efficiency
 258 table created by Harsha (DocDB 11467-v4).

259 We also calculated hit distributions for each hodoscope paddle and shown below in Figure
 260 21.

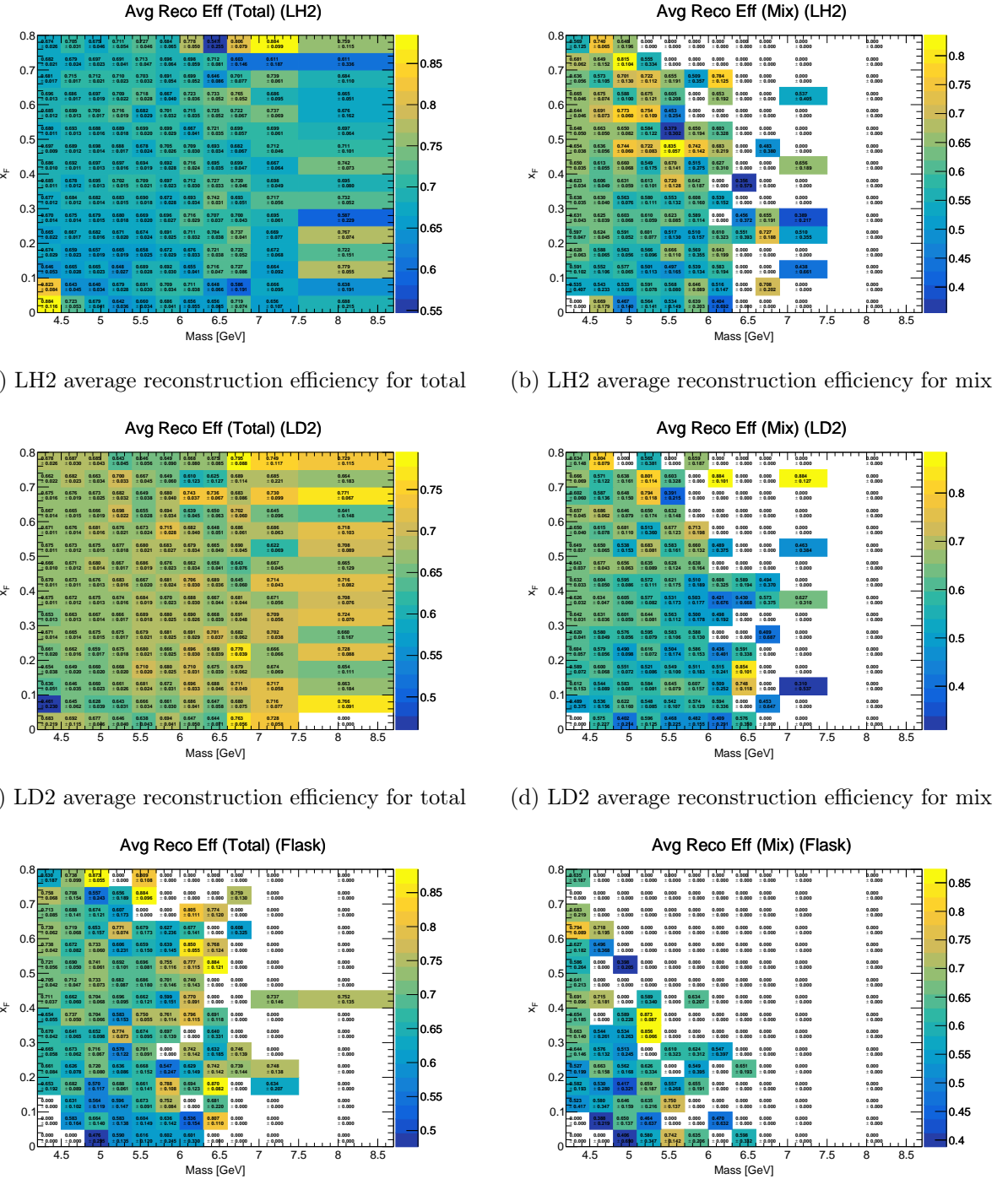


Figure 19: Average Reconstruction Efficiencies calculated each kinematic bin with the propagated uncertainties.

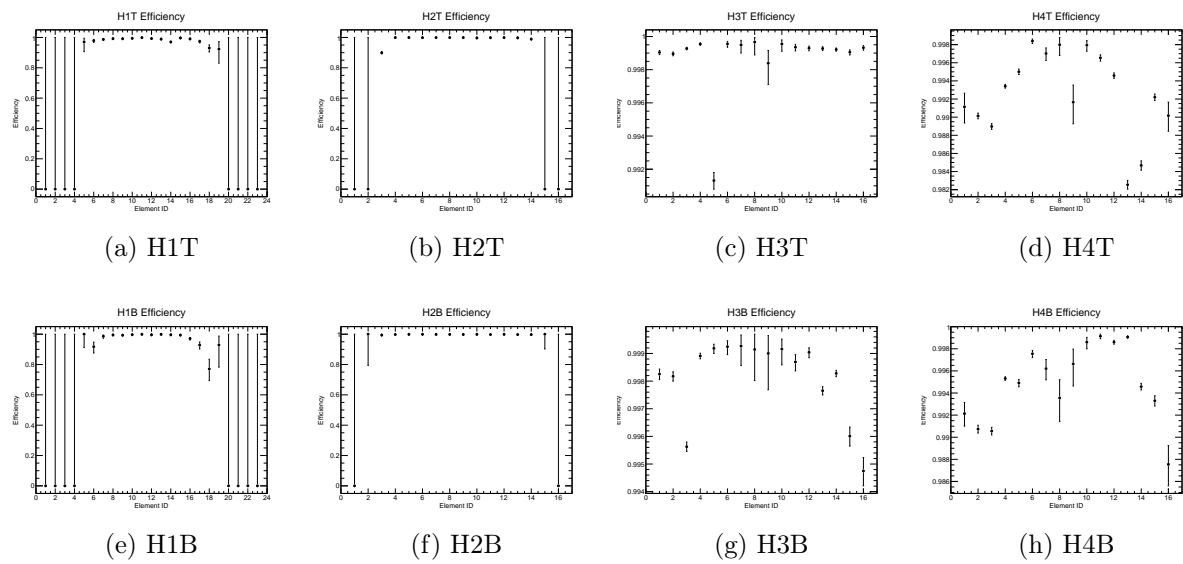


Figure 20: Hodoscope Paddle Efficiencies calculated in each plane.

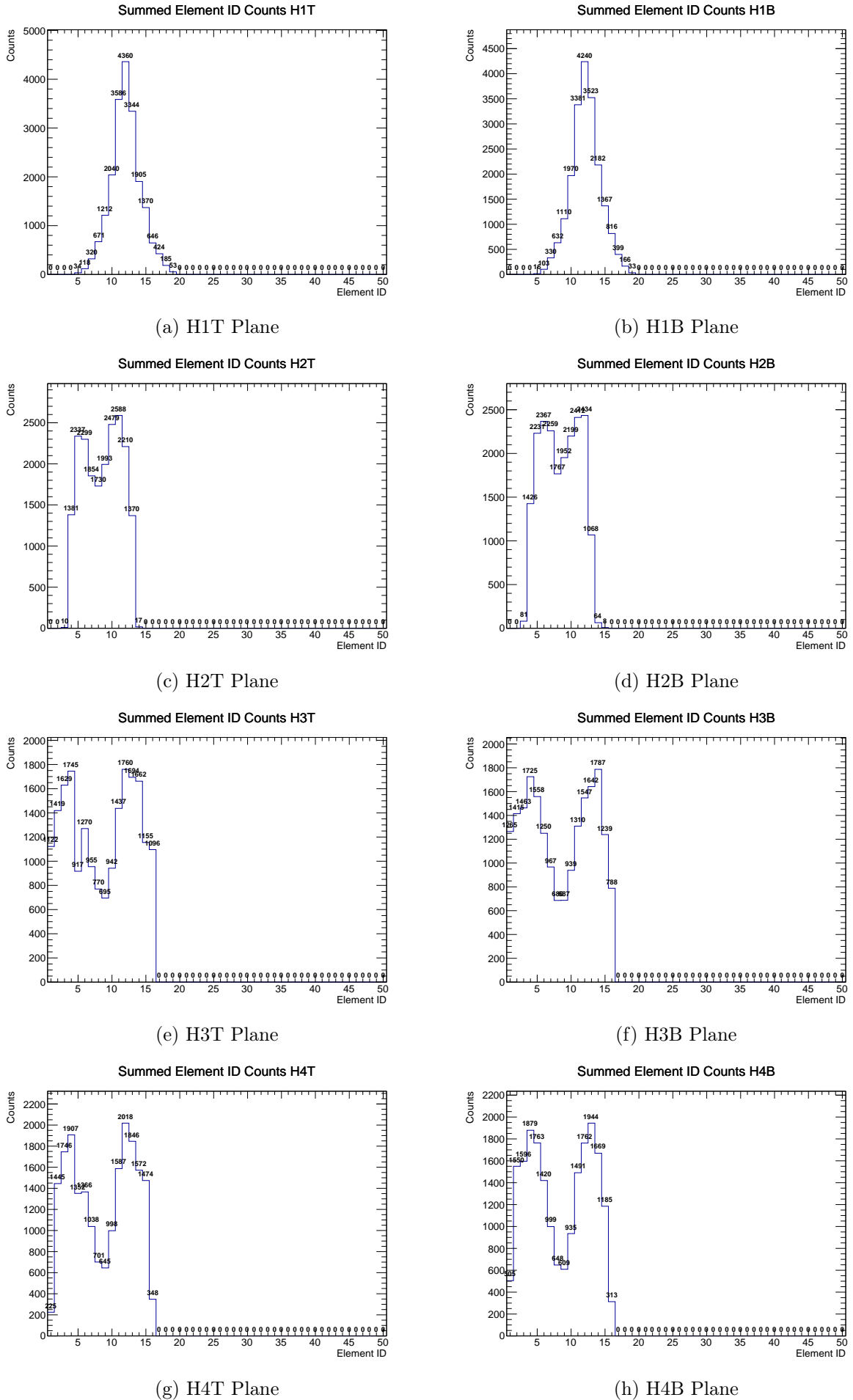


Figure 21: Hodoscope Paddle hit distributions arranged by Plane (Rows 1-4), Top vs Bottom.

262 The average hodoscope efficiency, $\langle \epsilon_{\text{hodo}} \rangle$, along with propagated uncertainty, is calculated
 263 for each kinematic bin. 2-D plots are shown below in Figure 22.

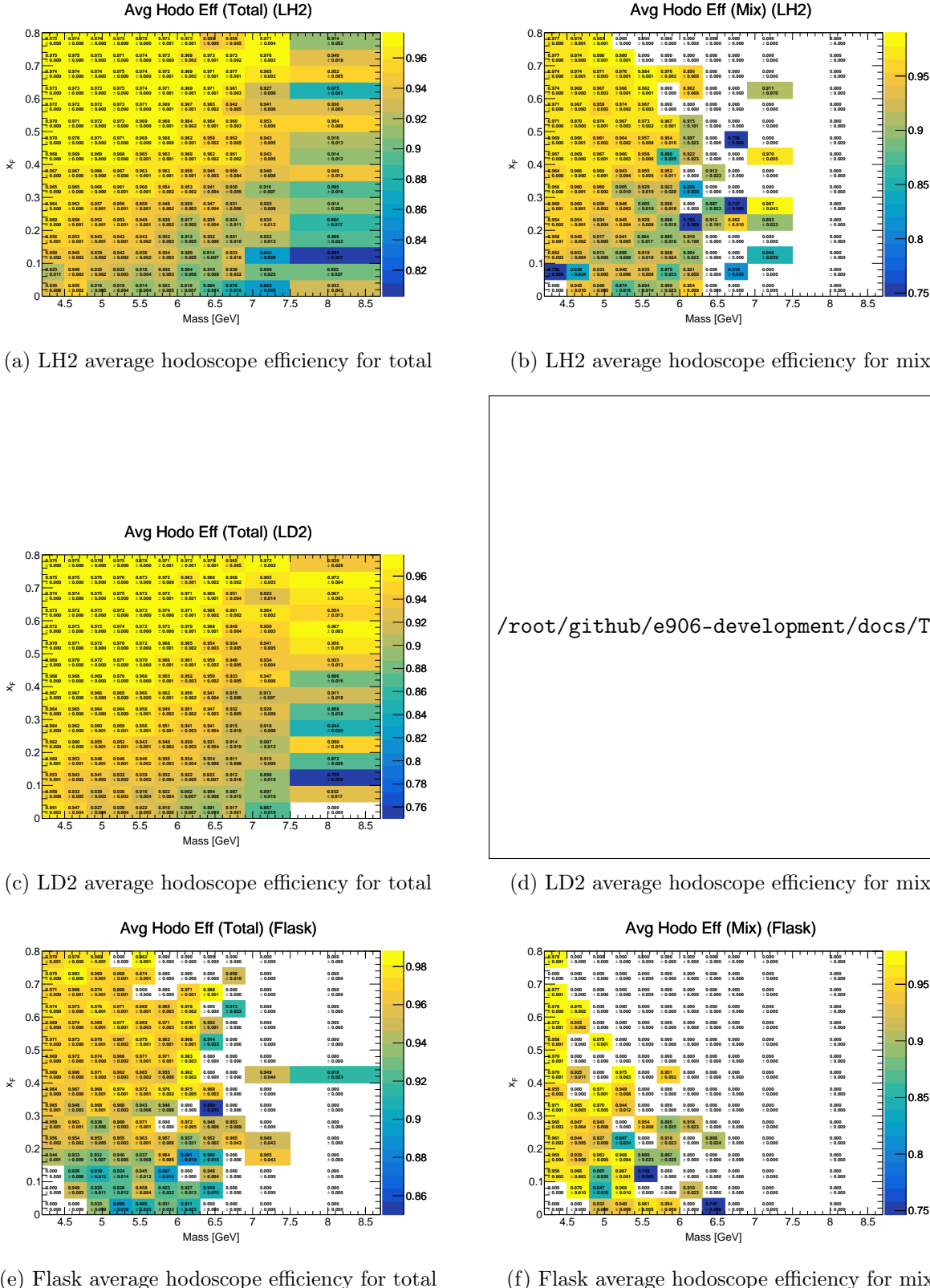


Figure 22: Average Hodoscope Efficiencies calculated each kinematic bin with the propagated uncertainties.

264 6 Total Efficiency Correction

265 The total efficiency correction ϵ_{total} is calculated on an event-by-event basis as the product of
266 the reconstruction and hodoscope efficiencies:

$$\epsilon_{\text{total}} = \epsilon_{\text{reco}} \times \epsilon_{\text{hodo}} \quad (14)$$

267 The average total efficiencies for the total and mixed event yields, along with their propagated
268 uncertainties, are calculated for each kinematic bin and are shown below in Figure 23.

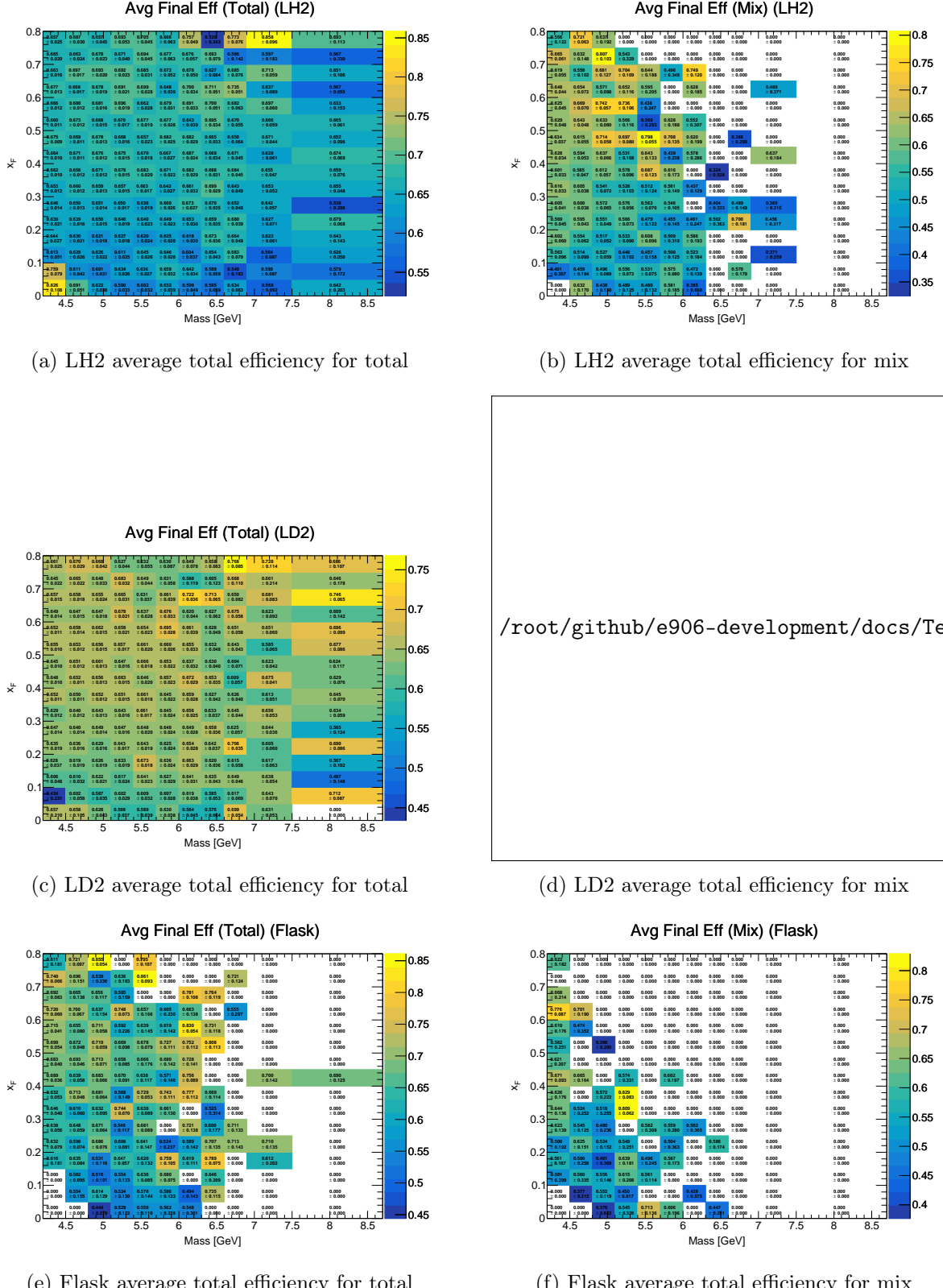


Figure 23: Average total Efficiencies calculated each kinematic bin with the propagated uncertainties.

269 7 Determination of Corrected Yields

270 With the average total efficiencies determined, we extract the corrected yields by calculating the
271 average signal efficiency correction using the following equation:

$$\langle \epsilon_{\text{sig}} \rangle = \frac{1}{Y_{\text{total}} - Y_{\text{mix}}} [\epsilon_{\text{total}} Y_{\text{total}} - \epsilon_{\text{mix}} Y_{\text{mix}}] \quad (15)$$

272 We then apply this correction factor to determine the final background-subtracted yield for the
273 signal:

$$Y_{\text{corrected}} = \frac{Y_{\text{total}} - Y_{\text{mix}}}{\langle \epsilon_{\text{sig}} \rangle} \quad (16)$$

274 The resulting average signal efficiency corrections and the corrected signal yields for each target
275 configuration are presented in Figure 24.

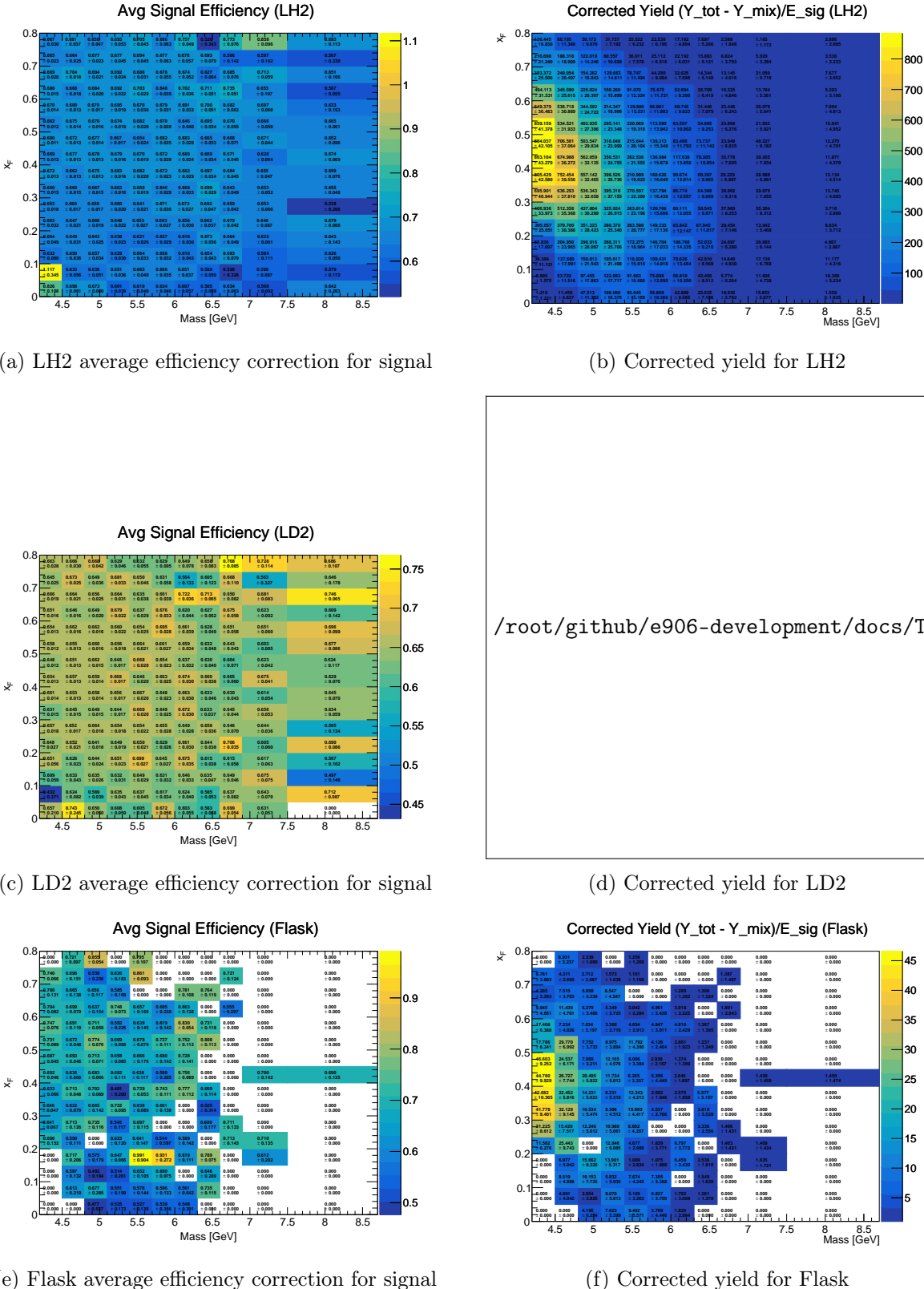


Figure 24: Average efficiency correction for signal and final corrected yields.

276 **8 Appendix: Event Selection Criteria (Chuck Cuts)**

277 The event selection criteria, commonly referred to as “Chuck Cuts,” are designed to select high-
 278 quality dimuon events originating from the target while rejecting backgrounds from the beam
 279 dump, upstream interactions, and cosmic rays. The cuts are applied at three levels: single track
 280 quality, dimuon vertex/kinematics, and detector occupancy.

281 In the following tables, the beam vertical offset is denoted as $y_{\text{beam}} = 1.6 \text{ cm}$.

282 **8.1 Single Track Cuts**

283 These cuts are applied individually to both the positive and negative muon tracks to ensure they
 284 are well-reconstructed and pass through the spectrometer magnet apertures correctly.

Table 1: Single track selection criteria.

Variable	Condition
Track Fit Quality	
Target χ^2	$\chi^2_{\text{target}} < 15$
Reduced χ^2	$\chi^2/(N_{\text{hits}} - 5) < 12$
Vertex Assumption	$\chi^2_{\text{target}} < 1.5 \times \chi^2_{\text{dump}}$ AND $\chi^2_{\text{target}} < 1.5 \times \chi^2_{\text{upstream}}$
Hits & Geometry	
Number of Hits	$N_{\text{hits}} > 13$
Station 1 Z-Momentum	$9 < p_{z,\text{st1}} < 75 \text{ GeV}/c$
Single Track Vertex z	$-320 < z_v < -5 \text{ cm}$
Aperture & Trajectory	
Radial pos. at target ($z \approx -130 \text{ cm}$)	$x^2 + (y - y_{\text{beam}})^2 < 320 \text{ cm}^2$
Radial pos. at dump ($z \approx 50 \text{ cm}$)	$16 < x^2 + (y - y_{\text{beam}})^2 < 1100 \text{ cm}^2$
Vertical Focusing	$y_{\text{st1}}/y_{\text{st3}} < 1$
Vertical Projection	$y_{\text{st1}} \cdot y_{\text{st3}} > 0$
Min Vertical Momentum	$ p_{y,\text{st1}} > 0.02 \text{ GeV}/c$
Momentum Conservation	
KMag Momentum Kick	$ p_{x,\text{st1}} - p_{x,\text{st3}} - 0.416 < 0.008 \text{ GeV}/c$
Vertical Bend (Null)	$ p_{y,\text{st1}} - p_{y,\text{st3}} < 0.008 \text{ GeV}/c$
Longitudinal (Null)	$ p_{z,\text{st1}} - p_{z,\text{st3}} < 0.08 \text{ GeV}/c$

285 **8.2 Dimuon Cuts**

286 After forming a dimuon pair, the following cuts ensure the vertex is valid and the kinematics
 287 fall within the trustworthy region of the spectrometer acceptance.

288 **8.3 Occupancy and Topology Cuts**

289 These cuts remove events with high detector activity (which complicates reconstruction) and en-
 290 sure the two muons pass through opposite sides of the spectrometer (the standard “top/bottom”
 291 trigger topology).

Table 2: Dimuon kinematic and vertex selection criteria.

Variable	Condition
Vertex Position	
Transverse Offset (x)	$ dx < 0.25 \text{ cm}$
Vertical Offset (y)	$ dy - y_{\text{beam}} < 0.22 \text{ cm}$
Radial Vertex	$dx^2 + (dy - y_{\text{beam}})^2 < 0.06 \text{ cm}^2$
Longitudinal Vertex (z)	$-280 < dz < -5 \text{ cm}$
Vertex Fit Quality	$\chi^2_{\text{dimuon}} < 18$
Vertex Consistency	$ \chi^2_{\text{trk1}} + \chi^2_{\text{trk2}} - \chi^2_{\text{dimuon}} < 2$
Kinematics	
Invariant Mass	$4.2 < M_{\mu\mu} < 8.8 \text{ GeV}/c^2$
Feynman- x	$-0.1 < x_F < 0.95$
Transverse Scaling x_T	$0.05 < x_T \leq 0.58$
Costh (Collins-Soper)	$ \cos \theta < 0.5$
Longitudinal Momentum	$38 < p_z < 116 \text{ GeV}/c$
Transverse Momentum limits	$ dp_x < 1.8 \text{ GeV}/c, dp_y < 2.0 \text{ GeV}/c$
Total p_T	$dp_x^2 + dp_y^2 < 5.0 \text{ (GeV}/c)^2$
Track Separation	$\text{sep} < 270 \text{ cm}$

Table 3: Occupancy and topological cuts.

Variable	Condition
Chamber Occupancy	
Drift Chamber 1 Hits	$D1 < 400$
Drift Chamber 2 Hits	$D2 < 400$
Drift Chamber 3 Hits	$D3 < 400$
Total Chamber Hits	$D1 + D2 + D3 < 1000$
Topology	
Opposite Quadrants	$y_{\text{st3}}^{\text{trk1}} \cdot y_{\text{st3}}^{\text{trk2}} < 0$
Total Hits on Tracks	$N_{\text{hits}}^{\text{trk1}} + N_{\text{hits}}^{\text{trk2}} > 29$
Station 1 Hits Sum	$N_{\text{hits, st1}}^{\text{trk1}} + N_{\text{hits, st1}}^{\text{trk2}} > 8$
Station 1 X-Sum	$ x_{\text{st1}}^{\text{trk1}} + x_{\text{st1}}^{\text{trk2}} < 42 \text{ cm}$

²⁹² 9 Appendix: Efficiency Plots

²⁹³ This appendix contains the efficiency studies used in this analysis. Figures 19, 22, and 21 show
²⁹⁴ the relevant efficiency and distribution maps.

295 **10 Appendix: Table of Systematic Errors**

Table 4: Detailed Systematic Error calculation for Bins in x_F and Mass

x_F Bin	Mass Bin (GeV)	Trigger Eff.	Acceptance	k-Tracker Eff.	Total Syst.
[0.00 - 0.05)	[4.50 - 4.80)	0.779025	1.873238	0.946767	2.238809
[0.00 - 0.05)	[4.80 - 5.10)	0.058272	0.052304	0.009351	0.078860
[0.00 - 0.05)	[5.10 - 5.40)	0.081048	0.047749	0.018181	0.095809
[0.00 - 0.05)	[5.40 - 5.70)	0.033849	0.013951	0.004059	0.036835
[0.00 - 0.05)	[5.70 - 6.00)	0.025896	0.009169	0.005236	0.027966
[0.00 - 0.05)	[6.00 - 6.30)	0.019771	0.006552	0.003990	0.021207
[0.00 - 0.05)	[6.30 - 6.60)	0.019741	0.006295	0.007003	0.021872
[0.00 - 0.05)	[6.60 - 6.90)	0.012449	0.004049	0.002978	0.013425
[0.00 - 0.05)	[6.90 - 7.50)	0.007375	0.001898	0.002170	0.007919
[0.00 - 0.05)	[7.50 - 8.70)	0.000946	0.000252	0.000628	0.001163
[0.05 - 0.10)	[4.50 - 4.80)	0.284881	0.378813	0.155516	0.498841
[0.05 - 0.10)	[4.80 - 5.10)	0.166470	0.128867	0.041569	0.214586
[0.05 - 0.10)	[5.10 - 5.40)	0.055664	0.025882	0.005169	0.061605
[0.05 - 0.10)	[5.40 - 5.70)	0.032285	0.011302	0.003966	0.034436
[0.05 - 0.10)	[5.70 - 6.00)	0.019937	0.006339	0.002229	0.021039
[0.05 - 0.10)	[6.00 - 6.30)	0.018107	0.005156	0.001957	0.018928
[0.05 - 0.10)	[6.30 - 6.60)	0.015415	0.004246	0.003557	0.016380
[0.05 - 0.10)	[6.60 - 6.90)	0.002562	0.000686	0.001166	0.002897
[0.05 - 0.10)	[6.90 - 7.50)	0.004064	0.000910	0.001134	0.004316
[0.05 - 0.10)	[7.50 - 8.70)	0.003523	0.000764	0.001074	0.003762
[0.10 - 0.15)	[4.50 - 4.80)	0.198459	0.182806	0.040656	0.272868
[0.10 - 0.15)	[4.80 - 5.10)	0.083380	0.040798	0.013031	0.093736
[0.10 - 0.15)	[5.10 - 5.40)	0.081948	0.031238	0.010558	0.088333
[0.10 - 0.15)	[5.40 - 5.70)	0.030329	0.009540	0.002815	0.031918
[0.10 - 0.15)	[5.70 - 6.00)	0.024458	0.006894	0.002083	0.025497
[0.10 - 0.15)	[6.00 - 6.30)	0.023572	0.006173	0.002268	0.024472
[0.10 - 0.15)	[6.30 - 6.60)	0.011184	0.002813	0.001083	0.011583
[0.10 - 0.15)	[6.60 - 6.90)	0.006021	0.001560	0.001047	0.006307
[0.10 - 0.15)	[6.90 - 7.50)	0.004337	0.000867	0.000718	0.004481
[0.10 - 0.15)	[7.50 - 8.70)	0.002871	0.000555	0.000388	0.002950
[0.15 - 0.20)	[4.50 - 4.80)	0.124062	0.075232	0.015770	0.145945
[0.15 - 0.20)	[4.80 - 5.10)	0.115363	0.046469	0.012767	0.125024
[0.15 - 0.20)	[5.10 - 5.40)	0.072817	0.024387	0.004930	0.076950
[0.15 - 0.20)	[5.40 - 5.70)	0.041137	0.011396	0.003480	0.042828
[0.15 - 0.20)	[5.70 - 6.00)	0.035444	0.009302	0.002872	0.036756
[0.15 - 0.20)	[6.00 - 6.30)	0.020001	0.004856	0.001682	0.020651
[0.15 - 0.20)	[6.30 - 6.60)	0.010531	0.002410	0.000921	0.010843
[0.15 - 0.20)	[6.60 - 6.90)	0.008260	0.001887	0.001449	0.008596
[0.15 - 0.20)	[6.90 - 7.50)	0.002937	0.000541	0.000443	0.003019
[0.15 - 0.20)	[7.50 - 8.70)	0.000973	0.000170	0.000400	0.001065
[0.20 - 0.25)	[4.20 - 4.50)	0.166120	0.120909	0.026450	0.207158
[0.20 - 0.25)	[4.50 - 4.80)	0.145103	0.071032	0.012123	0.162010
[0.20 - 0.25)	[4.80 - 5.10)	0.102147	0.034999	0.005624	0.108123
[0.20 - 0.25)	[5.10 - 5.40)	0.053289	0.015003	0.002962	0.055440
[0.20 - 0.25)	[5.40 - 5.70)	0.041865	0.010845	0.002727	0.043332

Cont'd on next page

Table 4: (Continued)

x_F Bin	Mass Bin (GeV)	Trigger Eff.	Acceptance	k-Tracker Eff.	Total Syst.
[0.20 - 0.25)	[5.70 - 6.00)	0.027889	0.006527	0.001469	0.028680
[0.20 - 0.25)	[6.00 - 6.30)	0.013039	0.002957	0.001025	0.013410
[0.20 - 0.25)	[6.30 - 6.60)	0.016485	0.003541	0.001461	0.016924
[0.20 - 0.25)	[6.60 - 6.90)	0.006353	0.001394	0.000605	0.006533
[0.20 - 0.25)	[6.90 - 7.50)	0.001365	0.000229	0.000204	0.001398
[0.20 - 0.25)	[7.50 - 8.70)	0.001336	0.000211	0.000136	0.001359
[0.25 - 0.30)	[4.20 - 4.50)	0.141343	0.072939	0.010257	0.159384
[0.25 - 0.30)	[4.50 - 4.80)	0.130167	0.051529	0.006463	0.140145
[0.25 - 0.30)	[4.80 - 5.10)	0.079605	0.023998	0.003471	0.083216
[0.25 - 0.30)	[5.10 - 5.40)	0.054612	0.014272	0.002683	0.056510
[0.25 - 0.30)	[5.40 - 5.70)	0.038571	0.009218	0.001867	0.039701
[0.25 - 0.30)	[5.70 - 6.00)	0.023376	0.005079	0.001591	0.023974
[0.25 - 0.30)	[6.00 - 6.30)	0.017654	0.003770	0.001225	0.018093
[0.25 - 0.30)	[6.30 - 6.60)	0.007693	0.001519	0.000560	0.007862
[0.25 - 0.30)	[6.60 - 6.90)	0.007726	0.001536	0.001007	0.007941
[0.25 - 0.30)	[6.90 - 7.50)	0.005124	0.000778	0.000489	0.005206
[0.25 - 0.30)	[7.50 - 8.70)	0.000519	0.000076	0.000209	0.000565
[0.30 - 0.35)	[4.20 - 4.50)	0.143223	0.062852	0.006469	0.156541
[0.30 - 0.35)	[4.50 - 4.80)	0.100283	0.033699	0.003193	0.105842
[0.30 - 0.35)	[4.80 - 5.10)	0.078522	0.020901	0.002863	0.081307
[0.30 - 0.35)	[5.10 - 5.40)	0.052272	0.012726	0.001692	0.053826
[0.30 - 0.35)	[5.40 - 5.70)	0.035353	0.007742	0.001569	0.036225
[0.30 - 0.35)	[5.70 - 6.00)	0.019840	0.004222	0.001174	0.020318
[0.30 - 0.35)	[6.00 - 6.30)	0.016108	0.003287	0.001254	0.016488
[0.30 - 0.35)	[6.30 - 6.60)	0.010060	0.002023	0.000634	0.010281
[0.30 - 0.35)	[6.60 - 6.90)	0.008018	0.001569	0.000793	0.008208
[0.30 - 0.35)	[6.90 - 7.50)	0.003694	0.000533	0.000421	0.003756
[0.30 - 0.35)	[7.50 - 8.70)	0.001747	0.000242	0.000186	0.001773
[0.35 - 0.40)	[4.20 - 4.50)	0.106457	0.037922	0.003043	0.113051
[0.35 - 0.40)	[4.50 - 4.80)	0.100531	0.029480	0.003146	0.104811
[0.35 - 0.40)	[4.80 - 5.10)	0.072502	0.018895	0.002326	0.074960
[0.35 - 0.40)	[5.10 - 5.40)	0.048131	0.010864	0.001538	0.049365
[0.35 - 0.40)	[5.40 - 5.70)	0.020800	0.004392	0.000837	0.021275
[0.35 - 0.40)	[5.70 - 6.00)	0.020491	0.004143	0.000980	0.020928
[0.35 - 0.40)	[6.00 - 6.30)	0.013363	0.002624	0.000720	0.013637
[0.35 - 0.40)	[6.30 - 6.60)	0.006047	0.001135	0.000396	0.006165
[0.35 - 0.40)	[6.60 - 6.90)	0.005933	0.001107	0.000667	0.006072
[0.35 - 0.40)	[6.90 - 7.50)	0.003348	0.000459	0.000269	0.003390
[0.35 - 0.40)	[7.50 - 8.70)	0.001436	0.000183	0.000247	0.001469
[0.40 - 0.45)	[4.20 - 4.50)	0.099323	0.033040	0.002941	0.104716
[0.40 - 0.45)	[4.50 - 4.80)	0.075954	0.020641	0.002128	0.078738
[0.40 - 0.45)	[4.80 - 5.10)	0.055286	0.012835	0.001577	0.056778
[0.40 - 0.45)	[5.10 - 5.40)	0.038052	0.008469	0.001399	0.039008
[0.40 - 0.45)	[5.40 - 5.70)	0.028172	0.005715	0.000987	0.028763
[0.40 - 0.45)	[5.70 - 6.00)	0.015105	0.002920	0.000688	0.015400
[0.40 - 0.45)	[6.00 - 6.30)	0.014939	0.002774	0.000734	0.015213
[0.40 - 0.45)	[6.30 - 6.60)	0.012131	0.002291	0.000940	0.012381
[0.40 - 0.45)	[6.60 - 6.90)	0.005773	0.001030	0.000398	0.005877

Cont'd on next page

Table 4: (Continued)

x_F Bin	Mass Bin (GeV)	Trigger Eff.	Acceptance	k-Tracker Eff.	Total Syst.
[0.40 - 0.45)	[6.90 - 7.50)	0.002557	0.000353	0.000241	0.002593
[0.40 - 0.45)	[7.50 - 8.70)	0.000491	0.000061	0.000040	0.000496
[0.45 - 0.50)	[4.20 - 4.50)	0.078635	0.023049	0.002059	0.081969
[0.45 - 0.50)	[4.50 - 4.80)	0.067541	0.017403	0.001706	0.069768
[0.45 - 0.50)	[4.80 - 5.10)	0.053760	0.012443	0.001688	0.055207
[0.45 - 0.50)	[5.10 - 5.40)	0.028610	0.005965	0.001078	0.029245
[0.45 - 0.50)	[5.40 - 5.70)	0.020809	0.004172	0.000821	0.021239
[0.45 - 0.50)	[5.70 - 6.00)	0.015482	0.002928	0.000738	0.015774
[0.45 - 0.50)	[6.00 - 6.30)	0.010741	0.001999	0.000674	0.010946
[0.45 - 0.50)	[6.30 - 6.60)	0.011477	0.002063	0.000873	0.011694
[0.45 - 0.50)	[6.60 - 6.90)	0.004200	0.000754	0.000554	0.004303
[0.45 - 0.50)	[6.90 - 7.50)	0.004274	0.000573	0.000231	0.004319
[0.45 - 0.50)	[7.50 - 8.70)	0.000999	0.000121	0.000098	0.001011
[0.50 - 0.55)	[4.20 - 4.50)	0.091374	0.025832	0.003131	0.095007
[0.50 - 0.55)	[4.50 - 4.80)	0.038797	0.009116	0.001196	0.039872
[0.50 - 0.55)	[4.80 - 5.10)	0.035794	0.007792	0.001215	0.036652
[0.50 - 0.55)	[5.10 - 5.40)	0.025971	0.005366	0.000845	0.026533
[0.50 - 0.55)	[5.40 - 5.70)	0.017990	0.003538	0.000653	0.018346
[0.50 - 0.55)	[5.70 - 6.00)	0.010504	0.001914	0.000561	0.010691
[0.50 - 0.55)	[6.00 - 6.30)	0.006640	0.001204	0.000587	0.006773
[0.50 - 0.55)	[6.30 - 6.60)	0.007154	0.001324	0.000432	0.007288
[0.50 - 0.55)	[6.60 - 6.90)	0.004000	0.000731	0.000474	0.004094
[0.50 - 0.55)	[6.90 - 7.50)	0.001946	0.000254	0.000172	0.001970
[0.50 - 0.55)	[7.50 - 8.70)	0.001279	0.000149	0.000130	0.001294
[0.55 - 0.60)	[4.20 - 4.50)	0.049012	0.013093	0.001356	0.050748
[0.55 - 0.60)	[4.50 - 4.80)	0.045199	0.010565	0.001338	0.046436
[0.55 - 0.60)	[4.80 - 5.10)	0.031162	0.006899	0.001131	0.031937
[0.55 - 0.60)	[5.10 - 5.40)	0.019065	0.003784	0.000735	0.019451
[0.55 - 0.60)	[5.40 - 5.70)	0.011066	0.002143	0.000544	0.011285
[0.55 - 0.60)	[5.70 - 6.00)	0.007673	0.001386	0.000453	0.007810
[0.55 - 0.60)	[6.00 - 6.30)	0.003981	0.000698	0.000228	0.004048
[0.55 - 0.60)	[6.30 - 6.60)	0.003434	0.000599	0.000281	0.003497
[0.55 - 0.60)	[6.60 - 6.90)	0.003400	0.000586	0.000348	0.003468
[0.55 - 0.60)	[6.90 - 7.50)	0.002152	0.000282	0.000214	0.002181
[0.55 - 0.60)	[7.50 - 8.70)	0.000563	0.000065	0.000074	0.000571
[0.60 - 0.65)	[4.20 - 4.50)	0.040173	0.010809	0.001161	0.041617
[0.60 - 0.65)	[4.50 - 4.80)	0.024563	0.005615	0.000889	0.025212
[0.60 - 0.65)	[4.80 - 5.10)	0.017374	0.003688	0.000696	0.017775
[0.60 - 0.65)	[5.10 - 5.40)	0.011024	0.002225	0.000393	0.011254
[0.60 - 0.65)	[5.40 - 5.70)	0.007261	0.001362	0.000352	0.007396
[0.60 - 0.65)	[5.70 - 6.00)	0.006245	0.001139	0.000455	0.006364
[0.60 - 0.65)	[6.00 - 6.30)	0.004809	0.000872	0.000317	0.004898
[0.60 - 0.65)	[6.30 - 6.60)	0.003639	0.000641	0.000299	0.003707
[0.60 - 0.65)	[6.60 - 6.90)	0.001526	0.000273	0.000098	0.001554
[0.60 - 0.65)	[6.90 - 7.50)	0.001164	0.000147	0.000132	0.001181
[0.60 - 0.65)	[7.50 - 8.70)	0.000334	0.000038	0.000062	0.000342
[0.65 - 0.70)	[4.20 - 4.50)	0.024537	0.006446	0.000859	0.025384
[0.65 - 0.70)	[4.50 - 4.80)	0.018367	0.004297	0.000734	0.018877

Cont'd on next page

Table 4: (Continued)

x_F Bin	Mass Bin (GeV)	Trigger Eff.	Acceptance	k-Tracker Eff.	Total Syst.
[0.65 - 0.70)	[4.80 - 5.10)	0.010196	0.002166	0.000407	0.010432
[0.65 - 0.70)	[5.10 - 5.40)	0.008613	0.001753	0.000384	0.008798
[0.65 - 0.70)	[5.40 - 5.70)	0.008247	0.001614	0.000508	0.008419
[0.65 - 0.70)	[5.70 - 6.00)	0.004495	0.000836	0.000349	0.004586
[0.65 - 0.70)	[6.00 - 6.30)	0.002948	0.000528	0.000258	0.003006
[0.65 - 0.70)	[6.30 - 6.60)	0.000881	0.000156	0.000132	0.000905
[0.65 - 0.70)	[6.60 - 6.90)	0.001730	0.000297	0.000210	0.001768
[0.65 - 0.70)	[6.90 - 7.50)	0.002013	0.000264	0.000280	0.002049
[0.65 - 0.70)	[7.50 - 8.70)	0.004838	0.000546	0.017062	0.017743
[0.70 - 0.75)	[4.20 - 4.50)	0.018003	0.004826	0.000928	0.018662
[0.70 - 0.75)	[4.50 - 4.80)	0.014316	0.003395	0.000682	0.014729
[0.70 - 0.75)	[4.80 - 5.10)	0.009071	0.001949	0.000519	0.009293
[0.70 - 0.75)	[5.10 - 5.40)	0.005102	0.001052	0.000465	0.005230
[0.70 - 0.75)	[5.40 - 5.70)	0.002947	0.000565	0.000295	0.003015
[0.70 - 0.75)	[5.70 - 6.00)	0.002329	0.000432	0.000339	0.002393
[0.70 - 0.75)	[6.00 - 6.30)	0.002535	0.000456	0.000594	0.002644
[0.70 - 0.75)	[6.30 - 6.60)	0.001917	0.000343	0.000707	0.002072
[0.75 - 0.80)	[4.20 - 4.50)	0.012861	0.003466	0.001181	0.013372
[0.75 - 0.80)	[4.50 - 4.80)	0.002016	0.000478	0.000132	0.002076
[0.75 - 0.80)	[4.80 - 5.10)	0.019900	0.004388	0.022716	0.030517

²⁹⁶ **11 Appendix: Table of Cross-Section Values**

Table 5: Detailed cross-section calculation for Bins in x_F and Mass

x_F Bin	Mass Bin (GeV)	Bin Center (GeV)	Bin Average (GeV)	Cross-Section (nb-GeV 2)	stat. error (nb-GeV 2)	syst. error (nb-GeV 2)
[0.00, 0.05)	[4.5, 4.8)	4.650	4.740	5.266×10^0	3.059×10^0	2.239×10^0
[0.00, 0.05)	[4.8, 5.1)	4.950	5.006	3.939×10^{-1}	2.024×10^{-1}	7.886×10^{-2}
[0.00, 0.05)	[5.1, 5.4)	5.250	5.250	5.479×10^{-1}	1.864×10^{-1}	9.581×10^{-2}
[0.00, 0.05)	[5.4, 5.7)	5.550	5.512	2.288×10^{-1}	9.988×10^{-2}	3.684×10^{-2}
[0.00, 0.05)	[5.7, 6.0)	5.850	5.828	1.751×10^{-1}	7.393×10^{-2}	2.797×10^{-2}
[0.00, 0.05)	[6.0, 6.3)	6.150	6.178	1.336×10^{-1}	4.716×10^{-2}	2.121×10^{-2}
[0.00, 0.05)	[6.3, 6.6)	6.450	6.432	1.334×10^{-1}	4.608×10^{-2}	2.187×10^{-2}
[0.00, 0.05)	[6.6, 6.9)	6.750	6.749	8.415×10^{-2}	2.777×10^{-2}	1.343×10^{-2}
[0.00, 0.05)	[6.9, 7.5)	7.200	7.171	4.985×10^{-2}	1.846×10^{-2}	7.919×10^{-3}
[0.00, 0.05)	[7.5, 8.7)	8.100	7.914	6.397×10^{-3}	6.502×10^{-3}	1.163×10^{-3}
[0.05, 0.10)	[4.5, 4.8)	4.650	4.627	1.926×10^0	1.237×10^0	4.988×10^{-1}
[0.05, 0.10)	[4.8, 5.1)	4.950	4.944	1.125×10^0	3.799×10^{-1}	2.146×10^{-1}
[0.05, 0.10)	[5.1, 5.4)	5.250	5.251	3.763×10^{-1}	1.199×10^{-1}	6.160×10^{-2}
[0.05, 0.10)	[5.4, 5.7)	5.550	5.526	2.182×10^{-1}	6.716×10^{-2}	3.444×10^{-2}
[0.05, 0.10)	[5.7, 6.0)	5.850	5.865	1.348×10^{-1}	5.227×10^{-2}	2.104×10^{-2}
[0.05, 0.10)	[6.0, 6.3)	6.150	6.086	1.224×10^{-1}	4.329×10^{-2}	1.893×10^{-2}
[0.05, 0.10)	[6.3, 6.6)	6.450	6.408	1.042×10^{-1}	3.840×10^{-2}	1.638×10^{-2}
[0.05, 0.10)	[6.6, 6.9)	6.750	6.725	1.732×10^{-2}	1.601×10^{-2}	2.897×10^{-3}
[0.05, 0.10)	[6.9, 7.5)	7.200	7.125	2.747×10^{-2}	1.126×10^{-2}	4.316×10^{-3}
[0.05, 0.10)	[7.5, 8.7)	8.100	7.731	2.382×10^{-2}	1.045×10^{-2}	3.762×10^{-3}
[0.10, 0.15)	[4.5, 4.8)	4.650	4.685	1.342×10^0	4.340×10^{-1}	2.729×10^{-1}
[0.10, 0.15)	[4.8, 5.1)	4.950	4.956	5.636×10^{-1}	1.621×10^{-1}	9.374×10^{-2}
[0.10, 0.15)	[5.1, 5.4)	5.250	5.231	5.540×10^{-1}	1.229×10^{-1}	8.833×10^{-2}
[0.10, 0.15)	[5.4, 5.7)	5.550	5.500	2.050×10^{-1}	6.525×10^{-2}	3.192×10^{-2}
[0.10, 0.15)	[5.7, 6.0)	5.850	5.816	1.653×10^{-1}	5.186×10^{-2}	2.550×10^{-2}
[0.10, 0.15)	[6.0, 6.3)	6.150	6.139	1.593×10^{-1}	3.486×10^{-2}	2.447×10^{-2}
[0.10, 0.15)	[6.3, 6.6)	6.450	6.440	7.560×10^{-2}	2.478×10^{-2}	1.158×10^{-2}
[0.10, 0.15)	[6.6, 6.9)	6.750	6.746	4.070×10^{-2}	1.434×10^{-2}	6.307×10^{-3}
[0.10, 0.15)	[6.9, 7.5)	7.200	7.114	2.932×10^{-2}	1.115×10^{-2}	4.481×10^{-3}
[0.10, 0.15)	[7.5, 8.7)	8.100	7.838	1.941×10^{-2}	7.930×10^{-3}	2.950×10^{-3}
[0.15, 0.20)	[4.5, 4.8)	4.650	4.656	8.386×10^{-1}	2.133×10^{-1}	1.459×10^{-1}
[0.15, 0.20)	[4.8, 5.1)	4.950	4.920	7.798×10^{-1}	1.766×10^{-1}	1.250×10^{-1}
[0.15, 0.20)	[5.1, 5.4)	5.250	5.251	4.922×10^{-1}	1.046×10^{-1}	7.695×10^{-2}
[0.15, 0.20)	[5.4, 5.7)	5.550	5.520	2.781×10^{-1}	6.083×10^{-2}	4.283×10^{-2}
[0.15, 0.20)	[5.7, 6.0)	5.850	5.833	2.396×10^{-1}	5.007×10^{-2}	3.676×10^{-2}
[0.15, 0.20)	[6.0, 6.3)	6.150	6.138	1.352×10^{-1}	3.967×10^{-2}	2.065×10^{-2}
[0.15, 0.20)	[6.3, 6.6)	6.450	6.467	7.119×10^{-2}	2.568×10^{-2}	1.084×10^{-2}
[0.15, 0.20)	[6.6, 6.9)	6.750	6.748	5.584×10^{-2}	1.640×10^{-2}	8.596×10^{-3}
[0.15, 0.20)	[6.9, 7.5)	7.200	6.919	1.985×10^{-2}	1.594×10^{-2}	3.019×10^{-3}
[0.15, 0.20)	[7.5, 8.7)	8.100	7.632	6.576×10^{-3}	3.945×10^{-3}	1.065×10^{-3}
[0.20, 0.25)	[4.2, 4.5)	4.350	4.347	1.123×10^0	3.376×10^{-1}	2.072×10^{-1}
[0.20, 0.25)	[4.5, 4.8)	4.650	4.653	9.809×10^{-1}	2.274×10^{-1}	1.620×10^{-1}
[0.20, 0.25)	[4.8, 5.1)	4.950	4.953	6.905×10^{-1}	1.291×10^{-1}	1.081×10^{-1}
[0.20, 0.25)	[5.1, 5.4)	5.250	5.237	3.602×10^{-1}	7.549×10^{-2}	5.544×10^{-2}

Cont'd on next page

Table 5: (Continued)

x_F Bin	Mass Bin (GeV)	Bin Center (GeV)	Bin Average (GeV)	Cross-Section (nb-GeV 2)	stat. error (nb-GeV 2)	syst. error (nb-GeV 2)
[0.20, 0.25)	[5.4, 5.7)	5.550	5.539	2.830×10^{-1}	5.529×10^{-2}	4.333×10^{-2}
[0.20, 0.25)	[5.7, 6.0)	5.850	5.835	1.885×10^{-1}	3.880×10^{-2}	2.868×10^{-2}
[0.20, 0.25)	[6.0, 6.3)	6.150	6.157	8.814×10^{-2}	3.025×10^{-2}	1.341×10^{-2}
[0.20, 0.25)	[6.3, 6.6)	6.450	6.463	1.114×10^{-1}	2.832×10^{-2}	1.692×10^{-2}
[0.20, 0.25)	[6.6, 6.9)	6.750	6.761	4.295×10^{-2}	1.858×10^{-2}	6.533×10^{-3}
[0.20, 0.25)	[6.9, 7.5)	7.200	7.136	9.224×10^{-3}	1.130×10^{-2}	1.398×10^{-3}
[0.20, 0.25)	[7.5, 8.7)	8.100	7.634	9.030×10^{-3}	3.932×10^{-3}	1.359×10^{-3}
[0.25, 0.30)	[4.2, 4.5)	4.350	4.390	9.555×10^{-1}	2.055×10^{-1}	1.594×10^{-1}
[0.25, 0.30)	[4.5, 4.8)	4.650	4.653	8.799×10^{-1}	1.686×10^{-1}	1.401×10^{-1}
[0.25, 0.30)	[4.8, 5.1)	4.950	4.947	5.381×10^{-1}	9.957×10^{-2}	8.322×10^{-2}
[0.25, 0.30)	[5.1, 5.4)	5.250	5.243	3.692×10^{-1}	6.835×10^{-2}	5.651×10^{-2}
[0.25, 0.30)	[5.4, 5.7)	5.550	5.555	2.607×10^{-1}	5.198×10^{-2}	3.970×10^{-2}
[0.25, 0.30)	[5.7, 6.0)	5.850	5.840	1.580×10^{-1}	3.113×10^{-2}	2.397×10^{-2}
[0.25, 0.30)	[6.0, 6.3)	6.150	6.144	1.193×10^{-1}	2.663×10^{-2}	1.809×10^{-2}
[0.25, 0.30)	[6.3, 6.6)	6.450	6.466	5.200×10^{-2}	1.901×10^{-2}	7.862×10^{-3}
[0.25, 0.30)	[6.6, 6.9)	6.750	6.755	5.223×10^{-2}	1.888×10^{-2}	7.941×10^{-3}
[0.25, 0.30)	[6.9, 7.5)	7.200	7.107	3.464×10^{-2}	9.170×10^{-3}	5.206×10^{-3}
[0.25, 0.30)	[7.5, 8.7)	8.100	7.598	3.508×10^{-3}	2.544×10^{-3}	5.647×10^{-4}
[0.30, 0.35)	[4.2, 4.5)	4.350	4.355	9.682×10^{-1}	1.855×10^{-1}	1.565×10^{-1}
[0.30, 0.35)	[4.5, 4.8)	4.650	4.665	6.779×10^{-1}	1.236×10^{-1}	1.058×10^{-1}
[0.30, 0.35)	[4.8, 5.1)	4.950	4.947	5.308×10^{-1}	9.068×10^{-2}	8.131×10^{-2}
[0.30, 0.35)	[5.1, 5.4)	5.250	5.249	3.533×10^{-1}	6.288×10^{-2}	5.383×10^{-2}
[0.30, 0.35)	[5.4, 5.7)	5.550	5.542	2.390×10^{-1}	4.623×10^{-2}	3.623×10^{-2}
[0.30, 0.35)	[5.7, 6.0)	5.850	5.844	1.341×10^{-1}	2.975×10^{-2}	2.032×10^{-2}
[0.30, 0.35)	[6.0, 6.3)	6.150	6.133	1.089×10^{-1}	2.213×10^{-2}	1.649×10^{-2}
[0.30, 0.35)	[6.3, 6.6)	6.450	6.384	6.800×10^{-2}	2.056×10^{-2}	1.028×10^{-2}
[0.30, 0.35)	[6.6, 6.9)	6.750	6.741	5.420×10^{-2}	1.360×10^{-2}	8.208×10^{-3}
[0.30, 0.35)	[6.9, 7.5)	7.200	7.045	2.497×10^{-2}	6.858×10^{-3}	3.756×10^{-3}
[0.30, 0.35)	[7.5, 8.7)	8.100	7.919	1.181×10^{-2}	4.331×10^{-3}	1.773×10^{-3}
[0.35, 0.40)	[4.2, 4.5)	4.350	4.337	7.196×10^{-1}	1.297×10^{-1}	1.131×10^{-1}
[0.35, 0.40)	[4.5, 4.8)	4.650	4.640	6.796×10^{-1}	1.152×10^{-1}	1.048×10^{-1}
[0.35, 0.40)	[4.8, 5.1)	4.950	4.943	4.901×10^{-1}	8.446×10^{-2}	7.496×10^{-2}
[0.35, 0.40)	[5.1, 5.4)	5.250	5.238	3.254×10^{-1}	5.543×10^{-2}	4.937×10^{-2}
[0.35, 0.40)	[5.4, 5.7)	5.550	5.515	1.406×10^{-1}	3.281×10^{-2}	2.127×10^{-2}
[0.35, 0.40)	[5.7, 6.0)	5.850	5.832	1.385×10^{-1}	2.843×10^{-2}	2.093×10^{-2}
[0.35, 0.40)	[6.0, 6.3)	6.150	6.125	9.033×10^{-2}	2.093×10^{-2}	1.364×10^{-2}
[0.35, 0.40)	[6.3, 6.6)	6.450	6.446	4.087×10^{-2}	1.947×10^{-2}	6.165×10^{-3}
[0.35, 0.40)	[6.6, 6.9)	6.750	6.727	4.011×10^{-2}	1.084×10^{-2}	6.072×10^{-3}
[0.35, 0.40)	[6.9, 7.5)	7.200	7.175	2.263×10^{-2}	6.209×10^{-3}	3.390×10^{-3}
[0.35, 0.40)	[7.5, 8.7)	8.100	7.764	9.710×10^{-3}	3.761×10^{-3}	1.469×10^{-3}
[0.40, 0.45)	[4.2, 4.5)	4.350	4.351	6.714×10^{-1}	1.212×10^{-1}	1.047×10^{-1}
[0.40, 0.45)	[4.5, 4.8)	4.650	4.642	5.134×10^{-1}	8.883×10^{-2}	7.874×10^{-2}
[0.40, 0.45)	[4.8, 5.1)	4.950	4.934	3.737×10^{-1}	6.449×10^{-2}	5.678×10^{-2}
[0.40, 0.45)	[5.1, 5.4)	5.250	5.231	2.572×10^{-1}	4.759×10^{-2}	3.901×10^{-2}
[0.40, 0.45)	[5.4, 5.7)	5.550	5.514	1.904×10^{-1}	3.491×10^{-2}	2.876×10^{-2}
[0.40, 0.45)	[5.7, 6.0)	5.850	5.854	1.021×10^{-1}	2.355×10^{-2}	1.540×10^{-2}
[0.40, 0.45)	[6.0, 6.3)	6.150	6.176	1.010×10^{-1}	2.152×10^{-2}	1.521×10^{-2}

Cont'd on next page

Table 5: (Continued)

x_F Bin	Mass Bin (GeV)	Bin Center (GeV)	Bin Average (GeV)	Cross-Section (nb-GeV 2)	stat. error (nb-GeV 2)	syst. error (nb-GeV 2)
[0.40, 0.45)	[6.3, 6.6)	6.450	6.422	8.200×10^{-2}	1.722×10^{-2}	1.238×10^{-2}
[0.40, 0.45)	[6.6, 6.9)	6.750	6.751	3.902×10^{-2}	9.905×10^{-3}	5.877×10^{-3}
[0.40, 0.45)	[6.9, 7.5)	7.200	7.100	1.729×10^{-2}	8.435×10^{-3}	2.593×10^{-3}
[0.40, 0.45)	[7.5, 8.7)	8.100	7.821	3.316×10^{-3}	4.877×10^{-3}	4.960×10^{-4}
[0.45, 0.50)	[4.2, 4.5)	4.350	4.344	5.316×10^{-1}	9.382×10^{-2}	8.197×10^{-2}
[0.45, 0.50)	[4.5, 4.8)	4.650	4.642	4.566×10^{-1}	7.742×10^{-2}	6.977×10^{-2}
[0.45, 0.50)	[4.8, 5.1)	4.950	4.940	3.634×10^{-1}	6.084×10^{-2}	5.521×10^{-2}
[0.45, 0.50)	[5.1, 5.4)	5.250	5.238	1.934×10^{-1}	3.633×10^{-2}	2.925×10^{-2}
[0.45, 0.50)	[5.4, 5.7)	5.550	5.523	1.407×10^{-1}	2.747×10^{-2}	2.124×10^{-2}
[0.45, 0.50)	[5.7, 6.0)	5.850	5.841	1.047×10^{-1}	2.125×10^{-2}	1.577×10^{-2}
[0.45, 0.50)	[6.0, 6.3)	6.150	6.135	7.260×10^{-2}	1.647×10^{-2}	1.095×10^{-2}
[0.45, 0.50)	[6.3, 6.6)	6.450	6.437	7.758×10^{-2}	1.612×10^{-2}	1.169×10^{-2}
[0.45, 0.50)	[6.6, 6.9)	6.750	6.741	2.839×10^{-2}	8.681×10^{-3}	4.303×10^{-3}
[0.45, 0.50)	[6.9, 7.5)	7.200	7.198	2.889×10^{-2}	7.053×10^{-3}	4.319×10^{-3}
[0.45, 0.50)	[7.5, 8.7)	8.100	7.828	6.752×10^{-3}	2.599×10^{-3}	1.011×10^{-3}
[0.50, 0.55)	[4.2, 4.5)	4.350	4.353	6.177×10^{-1}	1.029×10^{-1}	9.501×10^{-2}
[0.50, 0.55)	[4.5, 4.8)	4.650	4.620	2.623×10^{-1}	4.829×10^{-2}	3.987×10^{-2}
[0.50, 0.55)	[4.8, 5.1)	4.950	4.949	2.420×10^{-1}	4.259×10^{-2}	3.665×10^{-2}
[0.50, 0.55)	[5.1, 5.4)	5.250	5.246	1.756×10^{-1}	3.222×10^{-2}	2.653×10^{-2}
[0.50, 0.55)	[5.4, 5.7)	5.550	5.534	1.216×10^{-1}	2.718×10^{-2}	1.835×10^{-2}
[0.50, 0.55)	[5.7, 6.0)	5.850	5.843	7.100×10^{-2}	1.676×10^{-2}	1.069×10^{-2}
[0.50, 0.55)	[6.0, 6.3)	6.150	6.121	4.488×10^{-2}	1.451×10^{-2}	6.773×10^{-3}
[0.50, 0.55)	[6.3, 6.6)	6.450	6.417	4.836×10^{-2}	1.310×10^{-2}	7.288×10^{-3}
[0.50, 0.55)	[6.6, 6.9)	6.750	6.690	2.704×10^{-2}	7.906×10^{-3}	4.094×10^{-3}
[0.50, 0.55)	[6.9, 7.5)	7.200	7.135	1.315×10^{-2}	4.040×10^{-3}	1.970×10^{-3}
[0.50, 0.55)	[7.5, 8.7)	8.100	7.861	8.646×10^{-3}	3.042×10^{-3}	1.294×10^{-3}
[0.55, 0.60)	[4.2, 4.5)	4.350	4.348	3.313×10^{-1}	5.895×10^{-2}	5.075×10^{-2}
[0.55, 0.60)	[4.5, 4.8)	4.650	4.634	3.055×10^{-1}	5.112×10^{-2}	4.644×10^{-2}
[0.55, 0.60)	[4.8, 5.1)	4.950	4.951	2.106×10^{-1}	3.677×10^{-2}	3.194×10^{-2}
[0.55, 0.60)	[5.1, 5.4)	5.250	5.247	1.289×10^{-1}	2.334×10^{-2}	1.945×10^{-2}
[0.55, 0.60)	[5.4, 5.7)	5.550	5.524	7.481×10^{-2}	1.696×10^{-2}	1.129×10^{-2}
[0.55, 0.60)	[5.7, 6.0)	5.850	5.830	5.187×10^{-2}	1.452×10^{-2}	7.810×10^{-3}
[0.55, 0.60)	[6.0, 6.3)	6.150	6.118	2.691×10^{-2}	1.286×10^{-2}	4.048×10^{-3}
[0.55, 0.60)	[6.3, 6.6)	6.450	6.420	2.321×10^{-2}	9.228×10^{-3}	3.497×10^{-3}
[0.55, 0.60)	[6.6, 6.9)	6.750	6.697	2.299×10^{-2}	6.715×10^{-3}	3.468×10^{-3}
[0.55, 0.60)	[6.9, 7.5)	7.200	7.185	1.455×10^{-2}	4.465×10^{-3}	2.181×10^{-3}
[0.55, 0.60)	[7.5, 8.7)	8.100	7.799	3.803×10^{-3}	1.816×10^{-3}	5.711×10^{-4}
[0.60, 0.65)	[4.2, 4.5)	4.350	4.357	2.716×10^{-1}	4.774×10^{-2}	4.162×10^{-2}
[0.60, 0.65)	[4.5, 4.8)	4.650	4.666	1.660×10^{-1}	3.053×10^{-2}	2.521×10^{-2}
[0.60, 0.65)	[4.8, 5.1)	4.950	4.945	1.174×10^{-1}	2.239×10^{-2}	1.777×10^{-2}
[0.60, 0.65)	[5.1, 5.4)	5.250	5.240	7.452×10^{-2}	1.633×10^{-2}	1.125×10^{-2}
[0.60, 0.65)	[5.4, 5.7)	5.550	5.547	4.908×10^{-2}	1.178×10^{-2}	7.396×10^{-3}
[0.60, 0.65)	[5.7, 6.0)	5.850	5.815	4.222×10^{-2}	1.379×10^{-2}	6.364×10^{-3}
[0.60, 0.65)	[6.0, 6.3)	6.150	6.146	3.251×10^{-2}	1.119×10^{-2}	4.898×10^{-3}
[0.60, 0.65)	[6.3, 6.6)	6.450	6.406	2.460×10^{-2}	6.754×10^{-3}	3.707×10^{-3}
[0.60, 0.65)	[6.6, 6.9)	6.750	6.708	1.032×10^{-2}	8.032×10^{-3}	1.554×10^{-3}
[0.60, 0.65)	[6.9, 7.5)	7.200	7.225	7.869×10^{-3}	3.112×10^{-3}	1.181×10^{-3}

Cont'd on next page

Table 5: (Continued)

x_F Bin	Mass Bin (GeV)	Bin Center (GeV)	Bin Average (GeV)	Cross-Section (nb-GeV 2)	stat. error (nb-GeV 2)	syst. error (nb-GeV 2)
[0.60, 0.65)	[7.5, 8.7)	8.100	8.039	2.259×10^{-3}	1.368×10^{-3}	3.421×10^{-4}
[0.65, 0.70)	[4.2, 4.5)	4.350	4.324	1.659×10^{-1}	3.011×10^{-2}	2.538×10^{-2}
[0.65, 0.70)	[4.5, 4.8)	4.650	4.650	1.242×10^{-1}	2.342×10^{-2}	1.888×10^{-2}
[0.65, 0.70)	[4.8, 5.1)	4.950	4.923	6.892×10^{-2}	1.510×10^{-2}	1.043×10^{-2}
[0.65, 0.70)	[5.1, 5.4)	5.250	5.219	5.822×10^{-2}	1.511×10^{-2}	8.798×10^{-3}
[0.65, 0.70)	[5.4, 5.7)	5.550	5.535	5.575×10^{-2}	1.145×10^{-2}	8.419×10^{-3}
[0.65, 0.70)	[5.7, 6.0)	5.850	5.840	3.039×10^{-2}	7.325×10^{-3}	4.586×10^{-3}
[0.65, 0.70)	[6.0, 6.3)	6.150	6.125	1.993×10^{-2}	8.279×10^{-3}	3.006×10^{-3}
[0.65, 0.70)	[6.3, 6.6)	6.450	6.440	5.959×10^{-3}	6.988×10^{-3}	9.048×10^{-4}
[0.65, 0.70)	[6.6, 6.9)	6.750	6.734	1.170×10^{-2}	4.284×10^{-3}	1.768×10^{-3}
[0.65, 0.70)	[6.9, 7.5)	7.200	7.164	1.361×10^{-2}	4.073×10^{-3}	2.049×10^{-3}
[0.65, 0.70)	[7.5, 8.7)	8.100	7.654	3.270×10^{-2}	2.300×10^{-2}	1.774×10^{-2}
[0.70, 0.75)	[4.2, 4.5)	4.350	4.334	1.217×10^{-1}	2.425×10^{-2}	1.866×10^{-2}
[0.70, 0.75)	[4.5, 4.8)	4.650	4.635	9.677×10^{-2}	1.880×10^{-2}	1.473×10^{-2}
[0.70, 0.75)	[4.8, 5.1)	4.950	4.944	6.132×10^{-2}	1.289×10^{-2}	9.293×10^{-3}
[0.70, 0.75)	[5.1, 5.4)	5.250	5.257	3.449×10^{-2}	9.039×10^{-3}	5.230×10^{-3}
[0.70, 0.75)	[5.4, 5.7)	5.550	5.585	1.992×10^{-2}	6.850×10^{-3}	3.015×10^{-3}
[0.70, 0.75)	[5.7, 6.0)	5.850	5.829	1.574×10^{-2}	4.508×10^{-3}	2.393×10^{-3}
[0.70, 0.75)	[6.0, 6.3)	6.150	6.128	1.714×10^{-2}	5.156×10^{-3}	2.644×10^{-3}
[0.70, 0.75)	[6.3, 6.6)	6.450	6.475	1.296×10^{-2}	4.424×10^{-3}	2.072×10^{-3}
[0.75, 0.80)	[4.2, 4.5)	4.350	4.347	8.694×10^{-2}	1.875×10^{-2}	1.337×10^{-2}
[0.75, 0.80)	[4.5, 4.8)	4.650	4.615	1.363×10^{-2}	8.592×10^{-3}	2.076×10^{-3}
[0.75, 0.80)	[4.8, 5.1)	4.950	4.935	1.345×10^{-1}	7.332×10^{-2}	3.052×10^{-2}

²⁹⁷ 12 Appendix: Transverse Momentum Distributions

298 **References**

- 299 [1] S. D. Drell and T. M. Yan, Phys. Rev. Lett. 25, 316 (1970).
- 300 [2] DocDB 11448-v2, [https://seaquest-docdb.fnal.gov/cgi-bin/sso/RetrieveFile?
301 docid=11448&filename=eff_mix_corr.pdf&version=2](https://seaquest-docdb.fnal.gov/cgi-bin/sso/RetrieveFile?docid=11448&filename=eff_mix_corr.pdf&version=2)
- 302 [3] DocDB 11427, [https://seaquest-docdb.fnal.gov/cgi-bin/sso/RetrieveFile?
303 docid=11427&filename=reco_eff_kinematics.pdf&version=1](https://seaquest-docdb.fnal.gov/cgi-bin/sso/RetrieveFile?docid=11427&filename=reco_eff_kinematics.pdf&version=1)
- 304 [4] DocDB 11467-v4, [https://seaquest-docdb.fnal.gov/cgi-bin/sso>ShowDocument?
305 docid=11467](https://seaquest-docdb.fnal.gov/cgi-bin/sso>ShowDocument?docid=11467)
- 306 [5] DocDB 11322.